THESIS FOR THE DEGREE OF DOCTOR OF PHILOSOPHY

Optimal Coordination Methods for Autonomous Vehicles in Mixed Traffic

Muhammad Faris

Department of Electrical Engineering
Chalmers University of Technology
Gothenburg, Sweden, 2025

Optimal Coordination Methods for Autonomous Vehicles in Mixed Traffic

Muhammad Faris
ISBN 978-91-8103-300-7

Acknowledgements, dedications, and similar personal statements in this thesis, reflect the author's own views.

Doktorsavhandlingar vid Chalmers tekniska högskola
Ny serie nr 5757
ISSN 0346-718X

Department of Electrical Engineering
Chalmers University of Technology
SE-412 96 Gothenburg, Sweden
Phone: +46 (0)31 772 1000

Cover:
Vehicles in a mixed traffic intersection, with road manager and sensors

Printed by Chalmers Digital Printing
Gothenburg, Sweden, October 2025

Optimal Coordination Methods for Autonomous Vehicles in Mixed Traffic

Muhammad Faris
Department of Electrical Engineering
Chalmers University of Technology

Abstract

Connected and Automated Vehicles (CAVs) are projected to dominate traffic roads in the future due to their potential advantages in efficiency and safety. CAVs are equipped with sensors and onboard computers that allows them to perform coordination. The transition toward fully autonomous era will see a gradual replacement of legacy Human-Driven Vehicles (HDVs) creating mixed traffic environments. In such environments, the presence of HDVs can pose challenges to CAVs due to their uncertain behaviors and intentions. The particular concern of CAVs-HDVs interactions occurs at traffic intersections, where these road segments are responsible for the highest share of traffic jams and fatalities. Additionally, vehicle coordination in mixed traffic involves computationally difficult problems that cannot be solved in a tractable way.

This thesis presents optimization-based coordination strategies which builds upon mixed-platooning scheme and heuristic approaches. By utilizing the CAVs presence, the platooning strategy is implemented to partially control the HDVs. To retrieve initial intersection crossing order, a feasibility-enforcing Alternating Direction Methods of Multipliers (ADMM) is employed. Furthermore, an optimization-based heuristic is developed to efficiently evaluate reordering scenarios. The heuristic employs constraint-feasibility check and cost comparison techniques. Next, in an economic optimal coordination scenario, a sensitivity-based heuristic is implemented to further reduce computational loads by approximating Nonlinear Program (NLP) solutions. The numerical results demonstrate that these heuristics can achieve near-optimal solutions and be better than the alternatives while can be hundred times faster than the Mixed-Integer Program (MIP) solvers.

Keywords: Autonomous vehicles, mixed traffic, mixed integer optimization, model predictive control.

To my family, friends, and teachers

"Humankind cannot gain anything without first giving something in return. To obtain, something of equal value must be lost."

The Alchemy's Law of Equivalent Exchange
Fullmetal Alchemist

List of Publications

This thesis is based on the following publications:

[A] **Muhammad Faris**, Paolo Falcone, Mario Zanon, "A Sensitivity-Based Heuristic for Vehicle Priority Assignment at Intersections". Published in *IFAC World Congress*, Yokohama, Japan, July 2023.

[B] **Muhammad Faris**, Mario Zanon, Paolo Falcone, "CAVs Coordination at Intersections in Mixed Traffic Via Feasibility-Enforcing ADMM". Published in *IEEE International Conference on Intelligent Transportation Systems (ITSC)*, Edmonton, Canada, September 2024.

[C] **Muhammad Faris**, Mario Zanon, Paolo Falcone, "An Optimization-based Dynamic Reordering Heuristic for Coordination of Vehicles in Mixed Traffic Intersections". Published in *IEEE Transactions on Control Systems Technology*, 2024.

[D] **Muhammad Faris**, Mario Zanon, Paolo Falcone, "A Sensitivity-based Heuristic for Economic Optimal CAVs Coordination in Mixed Traffic at Intersections". Submitted to a peer-reviewed scientific journal.

Other publications by the author, not included in this thesis, are:

[E] **Muhammad Faris**, Paolo Falcone, Jonas Sjöberg, "Optimization-based coordination of mixed traffic at unsignalized intersections based on platooning strategy". Published in *IEEE Intelligent Vehicles Symposium (IV)*, Aachen, Germany, May 2022.

[F] **Muhammad Faris**, Mario Zanon, Paolo Falcone, "Approximation of MINLP Coordination for CAVs in Mixed Traffic Intersections via Sensitivity-based ADMM". Manuscript in preparation for submission.

Contents

Acknowledgments

A young man had arrived in Sweden after a long trip from Indonesia to do his PhD. On his first day, he came to the administrator asking for his supervisor's office. She replied,"He is not here...".

Time flies and the PhD journey of this (not-so-young-anymore) man is (nearing) done.

In the name of Allah, the Most Gracious, the Most Merciful.

First of all, I would like to thank my main supervisor, Professor Paolo Falcone, who has given me an opportunity to pursue PhD study at Chalmers. You have invested your time and energy not only to supervise technical matters but also to educate me in my quest to become a PhD. Thank you for showing me how to be critical and professional when it comes to research and manuscript writing. It has been an honor working under your supervision.

Next, I want to extend my gratitude toward my co-supervisor, Professor Mario Zanon, for all his guidance and help, all the way from ideas to coding. Thank you for your dedications in educating me and also the theoretical, practical knowledge you have patiently taught me. I wish we could eventually meet in person one day.

I further would like to thank Professor Jonas Sjöberg who has welcomed me in the Mechatronics group and took care of me during my time at Chalmers, especially during Covid time. I am also grateful to be teaching assistants to courses taught by Professor Jonas Fredriksson, Professor Nikolce Murgovski, and Professor Torsten Wik, which have enrinched my knowledge in systems, control, and mechatronics. I also thank Professor Balázs Kulcsár for insightful discussions.

I would like to thank Wallenberg AI, Autonomous Systems and Software Program (WASP) which have funded our research project and provided me with interesting courses, events and links to colleagues from different institutions. I am grateful to meet Terra within the WASP Autonomous Systems program, who has been a good colleague and friend along the way.

Next, I would like to especially thank Masoud who has taken care of me when I first came to Chalmers and provided me with many practical information to navigate the PhD life at E2. The special gratitude also goes to Rémi whose hands-on technical expertise helped me many times when I am stuck.

I am further grateful to meet Albert and Ahmet at Chalmers. Thank you for

inviting me to the company and for all the great lunches, fikas, dinners, etc. I also want to thank other E2 colleagues who have been really nice to me: Carl-Johan (my longest office room mate), Karim, Sondre, Huang, Yao, Godwin, Amal, Hasith, Angel, Yixiao, Anand, Erik, Stefan, Sten, Yizhou, Johannes, Ektor, Ivo, Ankit, Angelos, Maxi, Pavel, Rita, Nishant, Alvin, Constantine, Sabino, Gabriel, Ze, Mattia, Lorenzo, Francesco, Martina, Wenhao, Attila, Ludvig, Rikard, Kristian, Daniel, Lasse, Adam, Isac, Filip, Ying, Lei, Ilya, Christine, Quentin, and other colleagues in E2.

Also, I would like to thank my friends in Gothenburg: Victor, Iqbaal, Eka, Rahmatdi, Yanuar, Ridwan, Pandu, Ryah, Mas Adit, Mbak Nesia, Alif, Irsyad, Zahi, Andhika, Agus, Alam, Rosa, Abi, Dhania, Mbak Ninis, Dimas, Faisyal, Iwan, Aji, Alit, Widia, Fathur, Dhanes, Bintang, Badi, Ahmed, Martina for all the good times here and treating me like family.

I also want to extend my gratitude to my UGM colleagues: Pak Adha, Pak Dony, Mas Galang, Reka, Guntur for motivating me to pursue PhD study.

Last but not least, my big families in Indonesia: my parents, my brother, my parents-in-law, brothers- and sisters-in-law deserve special thanks for their unwavering supports.

Lastly, I will not be able to go far without my beloved wife, Annisa, whose dedications, sacrifices, and prayers have been unconditionally supporting me in this PhD journey.

Acronyms

ADMM:	Alternating Direction Methods of Multipliers
AL:	Augmented Lagrangian
AV:	Autonomous Vehicle
B&B:	Branch and Bound
CAV:	Connected Autonomous Vehicle
CZ:	Conflict Zone
EH:	Exact Heuristic
FCFS:	First-Come, First-Serve
HDV:	Human-Driven Vehicle
IM:	Intersection Manager
KKT:	Karush-Kuhn Tucker conditions
LICQ:	Linear Independence Constraint Qualification
MIP:	Mixed-Integer Program
MINLP:	Mixed-Integer Non Linear Program
MIQP:	Mixed-Integer Quadratic Program
MPC:	Model Predictive Control
OCP:	Optimal Control Problem
OMIQP:	Original Mixed-Integer Quadratic Program
SH:	Sensitivity-based Heuristic
SMIQP:	Simplified Mixed-Integer Quadratic Program
SOSC:	Second Order Sufficient Conditions
TTI:	Time-To-Intersection

Part I

Overview

CHAPTER 1

Introduction

1.1 Background

Autonomous vehicles (AVs) (or self-driving cars) are expected to heavily impact urban transportation in the coming decades, leading to reduced traffic operations costs and more economically efficient road transport [1]. In fact, AVs can potentially improve traffic performance by mitigating traffic congestion [2], increasing traffic flow [3], and reducing energy and fuel consumption [4]. On the other hand, AVs are expected to preserve, or improve, the safety level for passengers and the environment by reducing traffic accidents and fatalities [5]. To achieve such objectives, AV technology shall achieve the highest level of autonomy, eliminating the need for human drivers and conventional traffic signs [6]. Such a shift requires, among other things, the AVs to communicate seamlessly with other connected agents and infrastructure, leading to what are known as Connected Autonomous Vehicles (CAVs).

It is well-known that vehicles negotiating traffic junctions like, e.g., intersections, roundabouts [7] can cause congestion and accidents, more frequently than in other circumstances. Therefore, vehicle interactions are strictly regulated by right-of-way rules, traffic lights, and signs. However, these methods

can still fail, as human drivers can misinterpret or neglect traffic rules [8]. In contrast, CAVs can negotiate intersections by executing *coordination algorithms* that embed collision avoidance rules, thus very much reducing the risk of collisions and the congestion severity [9].

However, the path toward full penetration of CAVs must go through transition periods, where CAVs will coexist with HDVs [1]. Such mixed traffic challenges the coordination of CAVs as HDVs typically neither cooperate nor communicate [10]. Furthermore, the behavior of human drivers is uncertain and can be predicted to a limited extent only [11]. These issues can be particularly critical in the context of intersections, where approximately 90% of the accidents are due to wrong drivers' decisions [12]. Besides safety, the presence of HDVs can dramatically reduce the advantages introduced by AV technologies mentioned so far. Hence, the problem of coordinating CAVs in mixed traffic must be fully understood to develop and deploy coordination strategies.

Motivated by the above issues, this thesis primarily aims to study the impact of accommodating HDVs in CAVs coordination at unsignalized intersections and develop computationally efficient methods to safely perform (approximately) optimal coordination in mixed traffic scenarios.

1.2 Problem Formulation

The following research questions are investigated in this thesis

1. **Q1** How to indirectly control HDVs trajectories at unsignalized intersections using CAVs?
2. **Q2** How to optimally perform closed-loop CAVs coordination in mixed traffic with HDVs?
3. **Q3** How to obtain an approximate initial crossing order in a computationally efficient way?
4. **Q4** How to design an approximately optimal and computationally efficient heuristic method to address changes of crossing order (reordering) scenarios?
5. **Q5** How to formulate economic optimal (traffic and energy-efficient) coordination and perform it in a computationally efficient way?

1.3 Related Works

We next present a review of the literature that has addressed questions **Q1-Q5**.

CAVs coordination at intersections

The problem of coordinating vehicles at unsignalized intersections has initially focused on CAVs only. This problem has been extensively and thoroughly studied in [13]–[18]. Unsurprisingly, these studies show that coordinated CAVs lead to better traffic performance indices than, for example, traditional traffic lights. One of the important tasks in this context is determining the access to the intersection, i.e., *crossing order*, which is usually paired with techniques to avoid longitudinal and lateral collisions inside the conflict zone (CZ), which is the area of the junction where the vehicles' paths intersect. In general, the collision timeslot or safety distance.

Heuristic methods

The existing approaches to determining the crossing order can generally be categorized as either optimization-based or heuristic-based. Examples of such approaches are presented in [19], [20] where the original Mixed-Integer Nonlinear Program (MINLP) formulation of the vehicle coordination problem is simplified into a Mixed-Integer Quadratic Program (MIQP). Mixed-Integer Program (MIP) formulations are used in [17], [21] to manage intersections, such that collisions are prevented. Note that the crossing order problem is considered an *NP-hard* problem due to the presence of a discrete set of decisions [22], which implies that the resulting MIP problem can be *computationally intractable* or not be solvable within real-time constraints. These issues motivate research on computationally efficient heuristics as an alternative to MIP formulations.

One of the widely used heuristics is First-Come, First-Serve (FCFS). This approach is revealed in [17], [23], [24] to select the order based on the arrival or exit sequence at the intersection area and create a *virtual* safe distance between the incoming vehicles. However, this approach can be far from optimal as no optimization process is involved. The work in [25] suggests the use of predicted entry times to the CZ to get the crossing order. In [14], the authors propose

a heuristic that uses vehicle reachability analysis to calculate priorities that can be used to determine the order. In [26], a directed tree search method was used to efficiently find crossing orders and its application is extended to lane change. Moreover, a rule-based heuristic combined with timeslot or exit time minimization was developed in [16] and [27]. It can be noted that none of them compares and evaluates their approaches against MIP solvers so that their distance from optimality cannot be verified.

Albeit not in road traffic systems, alternative heuristic methods, such as Alternating Direction Methods of Multipliers (ADMM) [28], have been used to approximately solve MIQPs in various applications [29]–[32].

Mixed traffic environment

The approaches developed for fully automated problem settings are not specifically designed to deal with mixed traffic scenarios. The lack of mechanisms to accommodate the presence of HDVs motivates the recently increasing body of research on coordination in mixed traffic. In [33], a platooning strategy is implemented to regulate the HDVs behind it to increase traffic efficiency at intersections. A similar goal is pursued by [34] in which the deep reinforcement learning is applied to minimize intersection queueing. The platooning concept is also revealed in [35], [36] to regulate HDVs in generic highway settings. However, these works do not consider uncertainty factors stemming from human drivers. In [37], they consider stochasticity in human intention in the CAVs coordination at roundabouts, while in [38] the driver's intentions are learned by using a neural network to develop a multi-mode controller. The crossing order problem at unsignalized intersections within mixed-traffic settings is also considered, e.g., in [39] with its gradient-based optimization, in [23] with FCFS, and in [40] with Time-To-Intersection (TTI) method.

Economic coordination

In optimization-based methods, the velocity-tracking objective paired with acceleration/deceleration input has been widely applied, as in [41], [42]. Aside from such tracking objectives, economical-oriented objectives such as travel delays and fuel consumption minimization are discussed in, e.g., [39], [43]. However, they neglect the relevant nonlinearities within powertrain (engine) dynamics required to address the energy economy. The use of economic ob-

jectives with powertrain dynamics is demonstrated in [44], but the crossing order is not addressed there.

Reordering scenarios

Furthermore, some studies have focused on reordering problems where the crossing order can dynamically change. For example, [45] implemented a time-varying priority assignment by evaluating possible collisions from each vehicle. In [46], a negotiation-based priority approach was applied to coordinate CAVs, allowing rules to be negotiated during the auction phase based on the current states of the vehicles. Arrival/exit time minimization-based methods were used in [47], [48], and [40] to handle changing traffic flow. These methods sort the order based on current states or maximum possible acceleration of each vehicle.

1.4 Scope and Contributions

Scope: The traffic setting recommended here is the high penetration rate of CAVs. This ensures that the number of CAVs as *traffic actuators* is much higher than that of HDVs to guarantee performance advantages. Nevertheless, the proposed heuristics in this thesis can also work for scenarios with lower penetration rates. Additionally, it is assumed that the knowledge of the exact behavior model of the HDVs is not available to the CAVs. Other entities such as pedestrians or cyclists are not considered in this thesis.
Contributions: This thesis presents the following main contributions:

1. Formulation of a MIQP problem for a platooning-based CAVs optimal coordination in mixed traffic with HDVs at unsignalized intersections.

2. Feasibility-enforcing ADMM approach to efficiently retrieve initial crossing order.

3. An Exact optimization-based Heuristic (EH) framework inspired by a tailored B&B to efficiently address reordering scenarios.

4. Formulation of a MINLP problem with an emphasis on economically optimal CAVs coordination at mixed traffic.

5. Sensitivity-based Heuristic (SH) framework for computationally cheaper NLPs approximations used in reordering cases, both in small and general large traffic settings.

1.5 Thesis outline

This thesis consists of two parts. Part I contains seven chapters that serve as a self-contained summary and overview of the publications (papers) appended in Part II.

The remainder of Part I is organized as follows. Chapter 2 briefly revisits optimization and optimal control theories that are essential to understanding the remaining chapters. In Chapter 3, the vehicle types, model, and intersection environment used in this thesis are explained. The platooning strategy utilized to regulate HDVs is also introduced there. Next, Chapter 4 presents the formulation of CAVs coordination problem in mixed traffic, including the details on the objective functions and safety constraints. This is followed by the explanations on the proposed heuristic methods to obtain initial crossing order and address reordering. In Chapter 5, selected numerical results from the appended papers are discussed. Moreover, the papers are briefly summarized in Chapter 6. Finally, Chapter 7 concludes the work in this thesis.

CHAPTER 2

Optimization and Optimal Control

This chapter presents an overview of the optimization theory and tools used in this thesis. Section 2.1 introduces generic constrained optimization problems and sensitivity analysis tools. Section 2.2 discusses heuristics to (approximately) solve Mixed-Integer Problems (MIPs). Finally, Section 2.3 describes the constrained optimal control theory and methods

2.1 Nonlinear Optimization

Let us consider the following *nonlinear constrained optimization* problem

$$\min_{x} \quad f(x), \tag{2.1a}$$

$$\text{s.t.} \quad g_i(x) = 0, \qquad i = 1, ..., m, \tag{2.1b}$$

$$h_i(x) \leq 0, \qquad i = 1, ..., l, \tag{2.1c}$$

where $x \in \mathbb{R}^n$ and $f : \mathbb{R}^n \to \mathbb{R}$ are the vector of decision variables and objective (cost) function, respectively. $g_i : \mathbb{R}^n \to \mathbb{R}^m$ with $g = [g_1, ..., g_m]^\top$ and $h_i : \mathbb{R}^n \to \mathbb{R}^l$ with $h = [h_1, ..., h_l]^\top$ are the equality and inequality constraint

functions, respectively. Note that (2.1) can be turned into a *maximization* problem using a negative objective function, i.e., $-f$ and vice versa.

In this thesis, problem (2.1) is smooth and at least twice continuously differentiable, further denoted as Nonlinear Program (NLP). In NLP, f, g, h can be nonlinear, but there are some exceptions. If f is a quadratic function whereas g, h are affine functions, then (2.1) is a Quadratic Program (QP). Additionally, NLP is *convex* if their functions are convex, i.e.,

$$f(\theta x_1 + (1-\theta)x_2) \leq \theta f(x_1) + (1-\theta)f(x_2), \quad \theta \in [0,1], \tag{2.2}$$

and the functions g_i are *affine*.

Conditions for Optimality

Next, fundamental properties held by the solutions of NLP (2.1), and used in this thesis, are recalled.

Definition 1: (Feasibility) *x is feasible w.r.t.* (2.1) *if it satisfies* (2.1b), (2.1c), *i.e., $x \in \mathcal{X}$ where $\mathcal{X} = \{x \ : \ g(x) = 0, \ h(x) \leq 0\}$.*

Definition 2: (Minimum point) *$x^* \in \mathcal{X}$ is a global minimizer of* (2.1) *if $f(x^*) \leq f(x)$, $\forall x \in \mathcal{X}$. If* (2.1) *is non-convex, x^* can also be defined as a local minimizer where $x \in \mathcal{X}$ is a subset of the neighborhood around x^*.*

To establish optimality conditions for (2.1) and guarantee its continuity, the following definitions are introduced.

Definition 3: (Linear Independence Constraint Qualification (LICQ)) *If $\nabla_x g(^*)$ and $\nabla_x h_{\mathcal{A}}(^*)$ are linearly independent, LICQ holds at x^*. The set $\mathcal{A}$ denotes the set of active constraints, i.e., $h_{\mathcal{A}}(x^*) = 0$, and $h_{\bar{\mathcal{A}}}(x^*) < 0$, where $\bar{\cdot}$ denotes the complement of a set.*

For other types of constraint qualifications, one may refer to [49]. The point $x \in \mathcal{X}^*$ is regular for the NLP (2.1) if it fulfills a constraint qualification such as LICQ.

Definition 4: (Augmented Lagrangian) *For the NLP* (2.1), *we define the Lagrangian function*

$$\mathcal{L} = f(x) + \lambda^\top g(x) + \mu_{\mathcal{A}}^\top h_{\mathcal{A}}(x), \tag{2.3}$$

where $\lambda \in \mathbb{R}^m, \mu \in \mathbb{R}^l$ are column vectors containing the *dual variables* (Lagrange multipliers) associated with g and h, respectively.

The first-order necessary conditions to the optimality of NLP (2.1) is described as follows.

Theorem 1: (Karush-Kuhn-Tucker (KKT) conditions) *If x^* is regular, then there exist vectors λ^*, μ^* such that*

$$\nabla_x \mathcal{L}(x^*, \lambda^*, \mu^*) = 0 \tag{2.4a}$$
$$g(x^*) = 0 \tag{2.4b}$$
$$h(x^*) \leq 0, \tag{2.4c}$$
$$h_{\mathcal{A}}(x^*) = 0, \tag{2.4d}$$
$$\mu \geq 0, \tag{2.4e}$$

(2.4a) is the *stationary* condition. (2.4b) and (2.4c) are the *primal feasibility* conditions. (2.4d) is the *complementary slackness* and (2.4e) is the dual feasibility. Any (x^*, λ^*, μ^*) that satisfies KKT conditions (2.4) is considered a KKT point. Note that, for convex NLP (2.1), a KKT point x^* leads to a global minimum. For non-convex NLPs (2.1), sufficient conditions for optimality can be formulated to achieve sufficient conditions for local minimum [50]. Thus, Second-Order Sufficient Conditions (SOSC) are provided.

Theorem 2: (Second-Order Sufficient Conditions (SOSC)) *Let x^*, λ^*, μ^* satisfy the KKT conditions and LICQ holds. Consider a matrix $Z \in \mathbb{R}^n$ such that $\nabla_x g(x)^\top Z = 0, \nabla_x h_{\mathcal{A}}^\top Z = 0, Z \neq 0$. If*

$$Z^\top \nabla^2_{xx} \mathcal{L}(x^*, \lambda^*, \mu^*) Z > 0, \tag{2.5}$$

then SOSC hold.

Sensitivity Analysis

Let us consider the following *parametric* NLP

$$\min_x \quad f(x, p), \tag{2.6a}$$
$$\text{s.t.} \quad g(x, p) = 0, \tag{2.6b}$$
$$h(x, p) \leq 0, \tag{2.6c}$$

where $p \in \mathbb{R}^q$ is a *parameter*, and its augmented Lagrangian

$$\mathcal{L} = f(x,p) + \lambda^\top g(x,p) + \mu_{\mathcal{A}}^\top h_{\mathcal{A}}(x,p). \tag{2.7}$$

The primal-dual solution of (2.6) is thus a function of p, i.e.,

$$z(p) = [x^*(p)^\top, \lambda^*(p)^\top, \mu^*(p)^\top]^\top. \tag{2.8}$$

The KKT conditions for NLP (2.6) are

$$r(x^*,p) = \begin{bmatrix} \nabla_x \mathcal{L}(z^*,p) \\ g(x^*,p) \\ h_{\mathcal{A}}(x^*,p) \end{bmatrix} = 0. \tag{2.9}$$

Also, $h_{\mathcal{A}}(x^*,p)$ may contain *weakly active constraints*, that is, $h_i(x^*,p) = 0$ and $\mu_i^* = 0$, which is non-differentiable.

Furthermore, LICQ and SOSC are used to establish the following

Theorem 3: *If LICQ and SOSC hold at p, then $x^*(p)$ is continuous in the neighborhood of p. Furthermore, if there is no weakly active constraint, then $\nabla_p x^*(p)$ exists by the Implicit Function Theorem* [49].

By leveraging Theorem 3, an *approximated* parametric solution of (2.6), $\hat{x}^*(p)$, can be calculated by using $\nabla_p x^*(p)$, i.e., *sensitivities* and $x^*(\tilde{p})$, i.e., a minimizer obtained at an initial point with nominal parameter $\tilde{p}$, via the first-order Taylor approximation

$$\hat{x}^*(p) \approx x^*(\tilde{p}) + \nabla_p x^*(p)(p - \tilde{p}). \tag{2.10}$$

The sensitivity $\nabla_p x^*(p)$ is obtained from differentiation of KKT (2.9) matrix

$$\frac{\partial z}{\partial p} = -\left(\frac{\partial r(z,p)}{\partial z}\right)^{-1} \frac{\partial r(z,p)}{\partial p}, \tag{2.11}$$

where $\nabla_p x^*(p)$ are in the first n rows of $\frac{\partial z}{\partial p}$.

It is notable that (2.10) only yields a valid approximation $\hat{x}^*(p)$ of $x^*(\tilde{p})$ within a neighborhood of $\tilde{p}$ to which p belongs, and as long as the active constraints within $h_{\mathcal{A}}(x^*,p) = 0$ remains unchanged. As this is generally not the case for NLP (2.6), a *generalized tangential predictor* [51] can be utilized to approximate the change in the solution $\Delta x(p) := \hat{x}^*(p) - x^*(\tilde{p})$. The predictor

is defined by the following local QP

$$\min_{\Delta x} \quad \frac{1}{2}\Delta x^\top H \Delta x + b^\top \Delta x \tag{2.12a}$$
$$\text{s.t.} \quad g + \nabla_x g^\top \Delta x + \nabla_p g^\top \Delta p = 0, \tag{2.12b}$$
$$h + \nabla_x h^\top \Delta x + \nabla_p h^\top \Delta p \leq 0, \tag{2.12c}$$

where

$$H = \nabla^2_{xx} \mathcal{L}(z^*, \tilde{p}),$$
$$b = \nabla_x \mathcal{L}(z^*, \tilde{p}) + \nabla_{xp} \mathcal{L}(z^*, \tilde{p}) \Delta p.$$

As this single QP (2.12) only yields accurate predictions for relatively *small* Δp, the *predictor-corrector* method is required for generally *large* Δp.

Predictor-Corrector QP

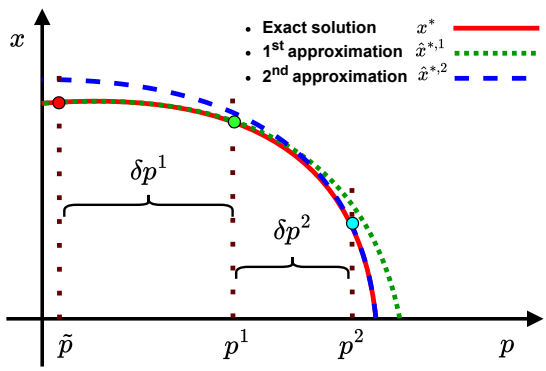

Figure 2.1: Sequential approximation of the predictor-corrector method.

Next, a concise explanation of the predictor-corrector method is reported, which resembles parametric sequential QP [52]. The fundamental idea is to split a large Δp, as in line 1 of Algorithm 1, into K smaller fixed steps δp (line 2) that are solved and integrated iteratively in a homotopy procedure

to obtain the next $\hat{x}^{*,j}, \lambda^{*,j}, \mu^{*,j}$ (lines 6-7). The routine is illustrated in Figure 2.1, where the short-dashed green curve represents the approximation of Δp calculated by the first iteration of QP (2.12) (line 5), which is used to reach p^1 and obtain $\hat{x}^{*,1}$. Using $\hat{x}^{*,1}$, the method next solves the QP to obtain the second approximation (long-dashed blue curve), which is used to reach the next point p^2 and obtain $\hat{x}^{*,2}$. This allows us to obtain a final approximate solution manifold $\hat{x}^*$ (line 11) that closely resembles the exact solution manifold x^*.

At each iteration j, the current parameter p^j along with f, g, h are updated to track the change of the solution curvature (line 8 of Algorithm 1). Alternatively, the sequence of points from $\tilde{p}$ to the final p in iteration n can be retrieved using $p^j = (1 - \zeta_j)\tilde{p} + \zeta_j p$, where $\zeta_j \in [0, 1]$. Since p enters the constraints linearly, the derivatives of g, h do not need to be updated. The approximated solution $\hat{x}^*$ can be used to, e.g., compute the cost function of NLP (2.6).

Algorithm 1 Predictor-corrector QP

Input: $\tilde{p}, p, x^*(\tilde{p})$
Output: $\hat{x}^*(p)$
1: Compute large step $\Delta p = p - \tilde{p}$
2: Compute small step $\delta p = \frac{\Delta p}{K}$
3: Set $p = \tilde{p}$, $\hat{x}^{*,0} = x^*$
4: **while** $j \leq K$ **do**
5: Solve QP (2.12)
6: Update primal solution $\hat{x}^{*,j} = \hat{x}^{*,j-1} + \Delta x$
7: Update dual variable $\lambda^{*,j} = \lambda^*_{\text{QP}}$, $\mu^{*,j} = \mu^*_{\text{QP}}$
8: $p^{j+1} = p^j + \delta p$ and update the sensitivities
9: $j = j + 1$
10: **end while**
11: Take $\hat{x}^*(p) = \hat{x}^{*,j-1}(p)$

2.2 Mixed-Integer Optimization

This thesis considers the problem where some of the decision variables are subjected to binary/integer constraints [53]. This leads to the Mixed-Integer Program (MIP) formulation of (2.1) which is non-convex. MIP can be further

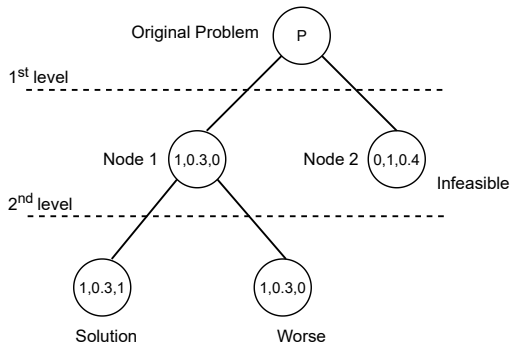

Figure 2.2: Search tree of a branch and bound

classified into Mixed-Integer QP (MIQP) and Mixed-Integer NLP (MINLP) depending on the objective function and/or the constraints.

Let us consider the following MIP problem

$$\min_{x^{\mathrm{c}},x^{\mathrm{b}}} \quad f(x^{\mathrm{c}},x^{\mathrm{b}}), \tag{2.13a}$$

$$\text{s.t.} \quad g(x^{\mathrm{c}},x^{\mathrm{b}}) = 0, \tag{2.13b}$$

$$h(x^{\mathrm{c}},x^{\mathrm{b}}) \leq 0, \tag{2.13c}$$

$$x^{\mathrm{b}} \in \{0,1\}^{n^{\mathrm{b}}} \tag{2.13d}$$

where $x^{\mathrm{c}} \in \mathbb{R}^{n^{\mathrm{c}}}, x^{\mathrm{b}}$ are the continuous and binary/integer variables, respectively. Due to constraint 2.13d, MIP (2.13) is considered as NP-hard [53]. That is, as the size of MIP (2.13) increases, the computational time to solve MIP (2.13) and obtain *exact* solutions $x^{\mathrm{c},*}, x^{\mathrm{b},*}$ can grow exponentially.

Next, selected methods used to (approximately) solve MIP problems are discussed.

Branch and Bound

The Branch and Bound (B&B) method is one of widely-used framework for solving integer or MIP problems. B&B divides the MIP (2.13) into N *subproblems* (nodes), e.g., by fixing some of x^{b}. The subproblems are ordered in

a tree structure as depicted in Figure 2.2. Then, it runs two subroutines to get the solutions and assesses the feasibility on each subproblem. The subroutines compute lower and upper bounds to retrieve a local minimum candidate. The upper bound can be found by choosing any binary point from a feasible area. One can make use of convex relaxation of the non-fixed binaries or duality theory to determine the lower bound.

The algorithm iteratively runs subproblems branching to search for a better solution in different levels and pruning infeasible or worse ones. The process stops when it cannot find any feasible solution or the error tolerance has been reached. The incumbent solution is then taken as the optimal solution. Due to the searching complexity, the procedure does not guarantee to get a global minimum and often it cannot be computationally efficient due to their enormous number of possible combinations.

There are many variations on B&B and its derivative methods applied in different MIP solvers due to their mainly different branching and pruning strategies, e.g., Branch-and-Cut [53].

Alternating Direction Methods of Multipliers

Alternating Direction Methods of Multipliers (ADMM) was originally developed to solve convex problems, mainly for distributed optimization and statistical learning applications [28]. ADMM with extensions have been applied as heuristics to solve non-convex or NP-hard problems [30], [32], [37].

ADMM iteratively performs primal problem minimization and multipliers updates. In particular, ADMM works in an alternating way when solving for primal and dual solutions. In the context of MIQP [29], ADMM can be used by rewriting (2.13) as

$$\min_{x} \quad f(x) + I_{\mathcal{X}}(x, y) \tag{2.14a}$$

$$\text{s.t.} \quad g(x) = 0, \tag{2.14b}$$

$$h(x) + h(y) = 0, \tag{2.14c}$$

where $x = [x^{\mathrm{c},\top}\ x^{\mathrm{b},\top}]^\top$ and $y \in \mathbb{R}^m$ is auxiliary variables. f is a quadratic objective function whereas $I_{\mathcal{X}}(x, y)$ denotes indicator function of $\mathcal{X}$. By adding auxiliary function $h(y)$, $h(x)$ is transformed into equality constraints.

To obtain near-optimal approximate solutions, ADMM can be designed with

dual loops. The outer loop generates random values within $\mathcal{X}$ to initialize the inner iterations, while in the inner loop, the following steps are carried out

$$\begin{bmatrix} x^{k+1/2} \\ y^{k+1/2} \end{bmatrix} := \operatorname{argmin} \left(f(x) + \frac{\rho}{2} ||g(x) + \lambda||_2^2 + \frac{\rho}{2} ||h(x) + h(y) + \mu||_2^2 \right) \tag{2.15a}$$

$$\begin{bmatrix} x^{k+1} \\ y^{k+1} \end{bmatrix} := \mathbf{\Pi} \left(\begin{bmatrix} x^{k+1/2} \\ y^{k+1/2} \end{bmatrix} + \begin{bmatrix} 0 & I \end{bmatrix} \begin{bmatrix} \lambda^k \\ \mu^k \end{bmatrix} \right) \tag{2.15b}$$

$$\begin{bmatrix} \lambda^{k+1} \\ \mu^{k+1} \end{bmatrix} := \begin{bmatrix} \lambda^k \\ \mu^k \end{bmatrix} + \begin{bmatrix} g(x) \\ h(x) + h(y) \end{bmatrix}, \tag{2.15c}$$

with $\mathbf{\Pi}$ denotes projection function to $\mathcal{X}$ which might not be unique in non convex settings and $\rho > \mathbb{R}^+$. In the case of x^{b}, $\mathbf{\Pi}$ can round it to the nearest binary/integer.

As there is no convergence guarantee to a local minimum, ADMM instead aims to find an approximate, feasible solution in a computationally faster way.

2.3 Optimal control

The optimal control approach combines control methods of dynamical systems and optimization. The goal is to find a sequence of optimized control actions, from an initial time t_0 to final time t_f, to drive a system trajectory by solving a constrained optimal control problem (OCP).

In the continuous-time domain, the OCP has the general form

$$\min_{x,u} \quad V(x(t_f)) + \int_{t_0}^{t_f} l(x(t), u(t)) \; dt \tag{2.16a}$$

$$\text{s.t.} \quad x(t_0) = \hat{x}_0, \tag{2.16b}$$

$$\dot{x}(t) = f(x(t), u(t)), \tag{2.16c}$$

$$h(x(t), u(t)) \leq 0, \tag{2.16d}$$

where x and u denote the the vector of states and input, respectively, while $\hat{x}_0$ is the initial state. v and l are the terminal and stage costs, respectively. f and h denote the dynamic model and the trajectory constraints.

In particular, the direct approaches to OCP are discussed next.

Direct Optimal Control

The direct approaches or direct optimal control works by parameterizing the infinite-dimensional variables x, u of continuous-time OCP (2.16) and approximating the problem using a finite-dimensional NLP (2.1), which can be solved using off-the-shelves solvers. In other words, "first discretize, then optimize".

The parameterization of u is performed by discretizing the input trajectory from t_0 to t_f using a uniform N intervals, i.e., $t_0, t_1, ..., t_N$ where $t_N = t_f$. In between, a piecewise constant policy is applied, i.e., $u(t) := u_k,\ \forall t \in [t_k, t_{k+1}]$, with $k \in [0, N-1]$ and $t_k = k\Delta t$ where Δk is the time interval. The discretized control input is $[u_1, u_2, ..., u_N]$.

In a similar manner, the *multiple shooting* technique can be applied to discretize $x(t)$ into the state vector $x = [x_0, x_1, ..., x_N]^\top$. To compute the solution of the dynamics (2.16c) and stage cost (2.16a), numerical integration is required, which can be explicit or implicit. Some of popular integrators include Euler, or Runge-Kutta methods.

The discretized OCP is as follows

$$\min_{x,u} \quad V(x_N) + \sum_{k=0}^{N-1} l_k(x_k, u_k)dt \tag{2.17a}$$

$$\text{s.t.} \quad x_0 = \hat{x}_0, \tag{2.17b}$$

$$x_{k+1} = F_k(x_k, u_k), \tag{2.17c}$$

$$h(x_k, u_k) \leq 0, \tag{2.17d}$$

where F_k and l_k are the discretized dynamics and stage cost, respectively. In this thesis, OCP (2.17) can be NLP or QP.

Model Predictive Control

By solving OCP (2.17) at t_k, $u_k^* \in [t_k, t_{k+N}]$ is obtained. One way here is to implement directly the resulting inputs for the whole future horizon, which is known as *open-loop control*. However, this may results in a poor performance as the measurement at future time $[t_{k+1}, t_{k+N}]$ are not considered in the open-loop scheme, i.e., the real x_k can be significantly different from the model (2.17c) due to model inaccuracies and uncertainty.

Therefore, *closed-loop* Model Predictive Control (MPC) is used instead where feedback mechanism is involved. The loop procedure is summarized

in the following steps

1. Obtain estimation/measurement of x_k at t_k
2. Solve OCP (2.17) and obtain $u_0^*, ..., u_N^*$
3. Implement u_0^*
4. Go back to step 1

u_0^* represents optimal input at the initial (current) time k and it is periodically updated every δt. The prediction horizon N is then also periodically shifted to follow the experiment/simulation time step.

CHAPTER 3

Vehicle Model and Environment

This chapter describes the types and modeling of vehicles and human driver behavior, along with mixed-traffic intersection settings applied in this thesis. Additionally, the mixed-platooning strategy is explained.

3.1 Vehicle Types

In this thesis, two types of vehicles are considered: Connected and Automated Vehicles (CAVs) and Human-Driven Vehicles (HDVs). A CAV is characterized by its ability to perform fully autonomous driving, i.e., without any human intervention, and to connect to other CAVs or road infrastructure to, e.g., share its information with other autonomous entities and coordinate their decisions accordingly. On the other hand, a HDV does not possess connectivity, which makes it unable to perform direct coordination.

Each vehicle considered here is assigned an integer index and belongs to either set of CAVs $\mathcal{N} := \{1, \dots, N\}$ or HDVs $\mathcal{M} := \{N+1, \dots, M\}$.

3.2 Vehicle Motion Model

In the literature, there are several motion models [54], [55] with different levels of detail, such as lateral & longitudinal motions, inertial effects, and powertrain. In this thesis, the longitudinal model is particularly selected as the path is predefined and the vehicle can follow it perfectly within the intersection area.

General form

A motion model of a vehicle with index $i \in \mathcal{N}, \mathcal{M}$ can be generally expressed as the following ordinary differential function

$$\dot{x}_i(t) = f(x_i(t), u_i(t)), \tag{3.1}$$

where the state vector $x_i(t) = [p_i(t), v_i(t)]^\top \subseteq \mathbb{R}^2$ contains the longitudinal distance of vehicle i from its origin point and its longitudinal velocity. The time is $t \in \mathbb{R}_+$ and $u_i(t)$ is the input. Also, the vehicle motion starts from the given initial states $x_{i,0} = x_i^0$, and is subject to some physical limitations, e.g., maximum velocity and acceleration.

The continuous-time model (3.1) above can be translated into discrete time by using numerical integration over the interval $[t_k, t_{k+1}]$, of duration Δt, such that $k = \lfloor t/\Delta t \rfloor \in \mathbb{N}$ and $t_k = k\Delta t$. The discretization yields the following function

$$x_{i,k+1} = F(x_{i,k}, u_{i,k}), \tag{3.2}$$

where $x_{i,k}, u_{i,k}$ are the discrete-time state and input vectors, respectively.

Double-Integrator Kinematic

For the sake of simplicity, the kinematic motion of vehicle i is often described through a series of integrators, e.g., the linear double-integrator form

$$\dot{p}_i(t) = v_i(t), \tag{3.3a}$$
$$\dot{v}_i(t) = a_i(t), \tag{3.3b}$$

where $a_i(t)$ is the acceleration/deceleration. Since this continuous-time model is linear, it is often directly translated into its discrete-time equivalent with the state space form

$$x_{i,k+1} = Ax_{i,k} + Bu_{i,k}, \tag{3.4}$$

where $k = \lfloor t/\Delta t \rfloor \in \mathbb{N}$, Δt is the sampling interval, and the matrices are

$$A = \begin{bmatrix} 1 & \Delta t \\ 0 & 1 \end{bmatrix}, \quad B = \begin{bmatrix} \frac{1}{2}\Delta t^2 \\ \Delta t \end{bmatrix},$$

where the state vector contains the discrete-time position and velocity $x_{i,k} = [p_{i,k},\ v_{i,k}]^\top$ and the input $u_{i,k} = a_{i,k}$. The states and input are subject to the following velocity and acceleration/deceleration bounds

$$v^{\min} \leq v_{i,k} \leq v^{\max}, \tag{3.5a}$$
$$a^{\min} \leq u_{i,k} \leq a^{\max}, \tag{3.5b}$$

with $v^{\min} > 0$, as vehicle i cannot reverse.

Nonlinear Dynamics

Vehicle i's motion can be alternatively described by using the following nonlinear dynamics

$$\dot{p}_i(t) = v_i(t), \tag{3.6}$$
$$\dot{v}_i(t) = \frac{1}{m_i}(F_i^{\mathrm{d}}(t) - F_i^{\mathrm{b}}(t) - F_i^{\mathrm{a}}(t) - F_i^{\mathrm{r}}), \tag{3.7}$$

where m_i is the vehicle mass, and $F_i^{\mathrm{d}}(t)$, $F_i^{\mathrm{b}}(t)$, $F_i^{\mathrm{a}}(t)$, $F_i^{\mathrm{r}}(t)$ are the forces associated with the engine motor torque, mechanical braking, aerodynamic drag, and rolling resistance, respectively [55]. The vehicle states are $x_i(t) = [p_i(t), v_i(t)]^\top$. The aerodynamic drag and rolling forces are defined as

$$F_i^{\mathrm{a}}(t) := \frac{1}{2}\rho A_i C_i^{\mathrm{d}} v_i^2(t), \tag{3.8}$$
$$F_i^{\mathrm{r}} := m_i g C_i^{\mathrm{r}} \cos\alpha, \tag{3.9}$$

where g is the gravitational acceleration, ρ the air density, and A_i the vehicle front area; constants C_i^{r} and C_i^{d} are the rolling friction and aerodynamic drag

coefficients, respectively; and α is the road slope angle. For simplicity, $\alpha = 0$, although accounting for $\alpha \neq 0$ does not require significant changes. The propulsive force is obtained from the generated motor torque $\tau_i(t)$ as

$$F_i^{\mathrm{d}}(t) := \frac{G_i^{\mathrm{r}}}{r_i^{\mathrm{w}}}\tau_i(t), \tag{3.10}$$

where G_i^{r} is the gear ratio, and r_i^{w} is the wheel radius. Note that transmission losses are not considered here for the sake of simplicity, but can readily be introduced [44]. The control inputs are $u_i(t) = [\tau_i,\ F_i^{\mathrm{b}}]^\top$.

Next, the engine and braking systems are subject to the following limitations

$$\tau^{\min} \leq \tau_i(t) \leq \tau^{\max}, \tag{3.11a}$$
$$\omega^{\min} \leq \omega_i(t) \leq \omega^{\max}, \tag{3.11b}$$
$$F^{\mathrm{b,min}} \leq F^{\mathrm{b}}(t) \leq F^{\mathrm{b,max}}, \tag{3.11c}$$

where the motor rotational speed $\omega_i(t)$ is related to the vehicle speed through

$$v_i(t) = \frac{r_i^{\mathrm{w}}}{G_i^{\mathrm{r}}}\omega_i(t). \tag{3.12}$$

Here, $\tau^{\max}$, $\omega^{\max}$, and $F^{\mathrm{b,max}}$ denote the maximum motor torque, rotational speed, and braking force, respectively, while $\tau^{\min}$, $\omega^{\min}$, and $F^{\mathrm{b,min}}$ are the minimum motor torque, rotational speed, and braking force, respectively. For implementation purposes, (3.7) above can be discretized into (3.2).

Moreover, the limitations on vehicle model, i.e., (3.5) or (3.11) can be compactly collected in $h^{\mathrm{limit}}(x_{i,k}, u_{i,k}) \leq 0$.

3.3 HDV behavior model

Two different HDV behavior models are employed here, each for *prediction* and *simulation* purposes. The difference stems from the idea that the mismatches between prediction and simulation are acknowledged due to the assumption that information on HDV real behavior (model and parameter values) is not exactly known [56], [57]. For prediction, the least assumption model is utilized, while the switching model is applied in simulations.

Note that other alternative HDV models exist in the literature [58]–[60] and can be used here instead if needed.

Prediction

For prediction, HDV i's trajectory is modeled after the following switching of constant velocity and maximum deceleration model

$$v_{i,k+1} = v_{i,k} + \Delta t a_{i,k}, \quad k > 0, \ \forall \ i \in \mathcal{M}, \tag{3.13}$$

where

$$a_{i,k} = \begin{cases} 0, & a_{i,k-1} \geq 0, \quad (3.14a) \\ a^{\min}, & a_{i,k-1} < 0, \quad (3.14b) \end{cases}$$

where the $a^{\min}$ is the maximum deceleration. Case (3.14b) covers the case in which the HDV slows down at $k-1$ to account for the *worst-case* braking, whereas case (3.14a) covers the non-decelerating scenarios using the *constant* velocity model.

Simulation

In simulations (experiments), the following model is applied

$$a_{m,k} = \begin{cases} a^{\mathrm{a}} + \Delta a_{i,k} & \Delta p_{m,k} \geq \bar{d}, \quad m \in \mathcal{M} \\ a^{\mathrm{b}} + \Delta a_{i,k} & \Delta p_{m,k} < \bar{d}, \end{cases} \tag{3.15}$$

where $\bar{d}$ is the switching threshold and

$$a^{\mathrm{a}} = k^{\mathrm{v}}(v_{i,k} - v_i^{\mathrm{ref}}), \tag{3.16a}$$
$$a^{\mathrm{b}} = k^{\mathrm{p}}(\Delta p_{i,k} - d^{\mathrm{ref}}) + k^{\mathrm{d}}(v_{i,k} - v_{j,k}), \tag{3.16b}$$

which is a switch between a *velocity-tracking* and a *car-following* model. The weighting gains are $k^{\mathrm{v}}, k^{\mathrm{p}}, k^{\mathrm{d}}$. Next, v_i^{ref} is the reference speed and $\Delta p_{i,k} := p_{j,k} - p_{i,k}$, where vehicle j is immediately in front of i. To account for uncertainties arising from human drivers, the bounded perturbation $\Delta a_{i,k}$ is added.

In the case of (3.4), the input of HDV i, $u_{i,k}$, is simply the accelera-

tion/deceleration $a_{i,k}$. If (3.7) is applied instead, the resulting $a_{i,k}$ must be translated into motor torque/braking forces. It is assumed that the human driver does not hit the gas and brake pedals at the same time [61], and thus the motor torque and braking force for HDV i are computed as

$$\tau_{i,k} := \begin{cases} \frac{r_i^{\mathrm{w}}}{G_i^{\mathrm{r}}}(m_i a_{i,k} - F_{i,k}^{\mathrm{a}} - F^{\mathrm{r}}) & \text{if } a_{i,k} > 0, \\ 0 & \text{otherwise,} \end{cases} \tag{3.17}$$

$$F_{i,k}^{\mathrm{b}} := \begin{cases} 0 & \text{if } a_{i,k} > 0, \\ -(m_i a_{i,k} + F_{i,k}^{\mathrm{a}} + F^{\mathrm{r}}) & \text{otherwise.} \end{cases} \tag{3.18}$$

3.4 Intersection and conflict zones

All vehicles entering an intersection share a common area where their predefined paths may intersect defined as the Conflict Zone (CZ). For simplicity, a symmetric CZ is considered in the center of a two-lane, crossroad as illustrated in Figure 3.1, in which each vehicle's path stretches from p^{in} to p^{out}. The motivation for a single CZ here is due to the assumption that HDVs heading intentions during crossing are *not known*, hence the whole CZ is exclusively reserved when each vehicle crosses. For other assumptions and different types of intersections or larger intersections, multiple CZs, as e.g., in [13] or multiple conflict points [62] approaches can be accommodated here.

For simplicity, the center of the CZ is considered as the origin of the position of each vehicle. Each direction branch of the junction only has a pair of opposite lanes, and overtaking action between adjacent vehicles is not considered here. Additionally, an intersection manager (IM) is deployed to help with CAV coordination, which can be located either locally or in the cloud, by relying on wireless communication (5G or 6G).

3.5 Platooning strategy

In this thesis, our objective is to take advantage of the presence of CAVs to efficiently regulate the traffic at intersections in mixed-traffic environments. The main idea is that, by adapting the speed of CAVs approaching the intersection, the behavior of HDVs can be indirectly controlled to optimize the overall intersection energy and traffic efficiency while maintaining safety.

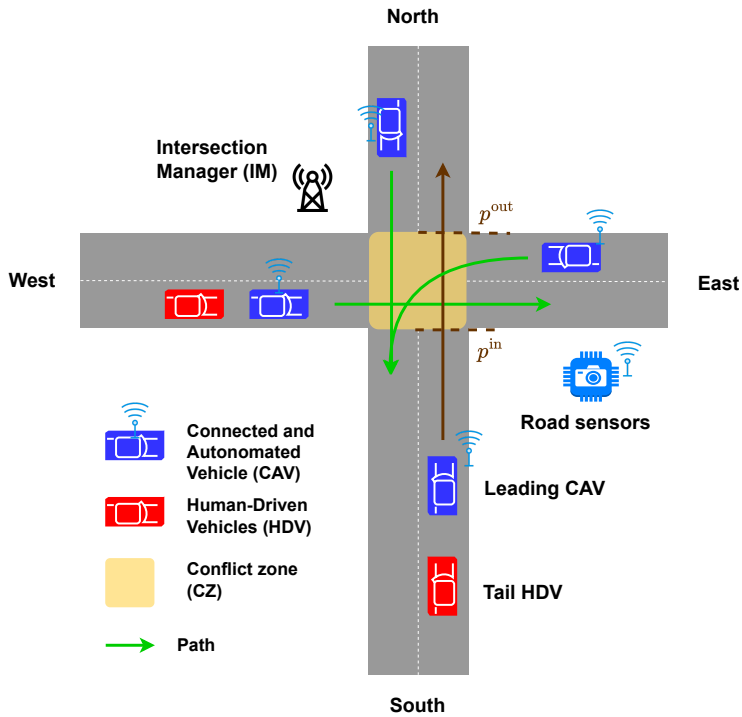

Figure 3.1: A mixed traffic intersection of CAVs and HDVs.

To that end, the mixed-platooning concept for mixed traffic intersection is introduced in Paper C. A platoon is described by a *leading* CAV followed by one or more HDVs, and thus the platoon length $l_{i,k}$ is measured from the position of the leader to that of the last vehicle (tail) in the platoon, as illustrated by the two-vehicle CAV-HDV platoon coming from the south in Figure 3.1. A vehicle that comes to the intersection without any succeeding or preceding vehicles is designated as an *isolated* (one-vehicle) platoon. When it comes to coordination, platoons are referred instead of individual vehicles.

Furthermore, all vehicle states and information (mass, coefficients, etc.) are available to the IM and CAVs, through, e.g., measurements and recognition from camera and road sensors. The IM is responsible for determining the members of a platoon by using, e.g., an inter-distance rule between adjacent vehicles or splitting the platoons in case it is deemed necessary.

CHAPTER 4

Coordination in Mixed Traffic Intersections

This chapter presents the discussion on the optimization problem formulation, including collision avoidance constraints and objective functions, required to perform safe and economic optimal coordination at unsignalized intersections in mixed traffic using platooning scheme.

Afterwards, the explanations on the proposed computationally-efficient heuristics methods to obtain approximate initial solutions and address reordering are provided.

4.1 Collision Avoidance Constraints

The collision avoidance constraints are implemented here to prevent collisions and hence maintain safety. They generally comprise two elements: lateral (side) and rear-end (longitudinal). The former is used to prevent collisions between platoons coming from different directions during crossing, whereas the latter is imposed between adjacent platoons. These constraints will be explained in detail next.

Lateral Collision Avoidance

To prevent lateral collisions at CZ between each pair of CAV-led platoons $i, j \in \mathcal{N}$, the following timeslot-based safety distance constraint is imposed

$$\text{if } t_j^{\text{out}} \leq t_i^{\text{in}} : \; p_{j,k} - l_{j,k} \geq p_{i,k} + d^{\min}, \; k \in [\underline{k}_j, \bar{k}_i], \tag{4.1a}$$
$$\text{if } t_i^{\text{out}} \leq t_j^{\text{in}} : \; p_{i,k} - l_{i,k} \geq p_{j,k} + d^{\min}, \; k \in [\underline{k}_i, \bar{k}_j], \tag{4.1b}$$

where $d^{\min}$ denotes the safety distance and $\underline{k}_c = \min(k \mid t_k \geq t_c^{\text{in}})$, $\bar{k}_c = \max(k \mid t_k \leq t_c^{\text{out}})$, $c \in \{i, j\}$. The timeslot variables $t_c^{\text{in}}, t_c^{\text{out}}, \underline{k}_c, \bar{k}_c$ satisfy

$$p_{c,\underline{k}_c} \geq p^{\text{in}}, \qquad p_{c,\bar{k}_c} \leq p^{\text{out}}, \tag{4.2a}$$
$$p_c(t_c^{\text{in}}) = p^{\text{in}}, \qquad p_c(t_c^{\text{out}}) = p^{\text{out}}. \tag{4.2b}$$

In words, constraint (4.1) describe two possible cases:

1. if $t_j^{\text{out}} \leq t_i^{\text{in}}$, then j occupies the CZ before i. Thus (4.1a) is imposed during $[\underline{k}_j, \bar{k}_i]$.

2. Conversely, $t_i^{\text{out}} \leq t_j^{\text{in}}$ indicates that i occupies the CZ before j. In this case, (4.1b) is imposed during $[\underline{k}_i, \bar{k}_j]$.

Additionally, the length of the preceding platoon $l_{c,k}$ is considered to ensure that the succeeding platoon is allowed to enter after the last vehicle of platoon c leaves CZ.

For implementation purpose of (4.1), binary indicators $\rho_{i,j,k}^{\text{in}}, \rho_{i,j,k}^{\text{out}} \in \{0, 1\}$ are introduced to activate the constraint within the selected timeslots, which rewrites the constraint as

$$(\rho_{i,j,k}^{\text{in}} - \rho_{i,j,k}^{\text{out}})(r_{i,j})(p_{j,k} - l_{j,k} - p_{i,k} - d^{\min}) \geq 0, \tag{4.3a}$$
$$(\rho_{i,j,k}^{\text{in}} - \rho_{i,j,k}^{\text{out}})(1 - r_{i,j})(p_{i,k} - l_{i,k} - p_{j,k} - d^{\min}) \geq 0, \tag{4.3b}$$

where $r_{i,j} \in \{0, 1\}$ is a binary variable that defines whether j crosses before i ($r_{i,j} = 1$) or the converse ($r_{i,j} = 0$).

The values of $\rho_{i,j,k}^{\text{in}}, \rho_{i,j,k}^{\text{out}}$ depend on the times at which the platoons occupy

the CZ, i.e., they must satisfy these activation/deactivation conditions

$$\rho^{\text{in}}_{i,j,k} \leq 1 + \frac{\bar{p}^{\text{in}}_k - p^{\text{in}}}{M^{\text{b}}}, \tag{4.4a}$$

$$\rho^{\text{in}}_{i,j,k} \geq \frac{\bar{p}^{\text{in}}_k - p^{\text{in}}}{M^{\text{b}}}, \tag{4.4b}$$

$$\rho^{\text{out}}_{i,j,k} \leq 1 + \frac{\bar{p}^{\text{out}}_k - p^{\text{out}}}{M^{\text{b}}}, \tag{4.4c}$$

$$\rho^{\text{out}}_{i,j,k} \geq \frac{\bar{p}^{\text{out}}_k - p^{\text{out}}}{M^{\text{b}}}, \tag{4.4d}$$

where,

$$\bar{p}^{\text{in}}_k = r_{i,j} p_{j,k} + (1 - r_{i,j}) p_{i,k}, \tag{4.5a}$$

$$\bar{p}^{\text{out}}_k = r_{i,j} p_{i,k} + (1 - r_{i,j}) p_{j,k}, \tag{4.5b}$$

and $M^{\text{b}} \in \mathbb{R}_{>0}$ is a sufficiently large constant. Conditions (4.4a) and (4.4b) are used to set $\rho^{\text{in}}_{i,j,k}$ to 0 when *either* of the platoons (i, j) (OR condition) is before p^{in} and to 1 otherwise. Similarly, conditions (4.4c) and (4.4d) are used to set $\rho^{\text{out}}_{i,j,k}$ to 0 or 1, respectively, when *both* platoons (AND condition) are before or after p^{out}. The implication of these conditions to (4.3) is illustrated in Figure 4.1, which shows the situation in which platoon i reaches the CZ before j, such that (4.3b) is selected and activated. After this time, $\rho^{\text{in}}_{i,j,k} = 1$. Similarly, after both vehicles have cleared the CZ, $\rho^{\text{out}}_{i,j,k} = 1$ and (4.3b) is no longer enforced.

Avoiding the multiplication of integer variables in (4.3) is convenient from a formulation standpoint, i.e., using Big-M [53], as shown next. Indeed, (4.3) can be rewritten as follows

$$M^{\text{b}}(1 - \rho^{\text{in}}_{i,j,k} + \rho^{\text{out}}_{i,j,k} + 1 - r_{i,j}) + p_{j,k} - l_{j,k} - p_{i,k} - d^{\min} \geq 0, \tag{4.6a}$$

$$M^{\text{b}}(1 - \rho^{\text{in}}_{i,j,k} + \rho^{\text{out}}_{i,j,k} + r_{i,j}) + p_{i,k} - l_{i,k} - p_{j,k} - d^{\min} \geq 0, \tag{4.6b}$$

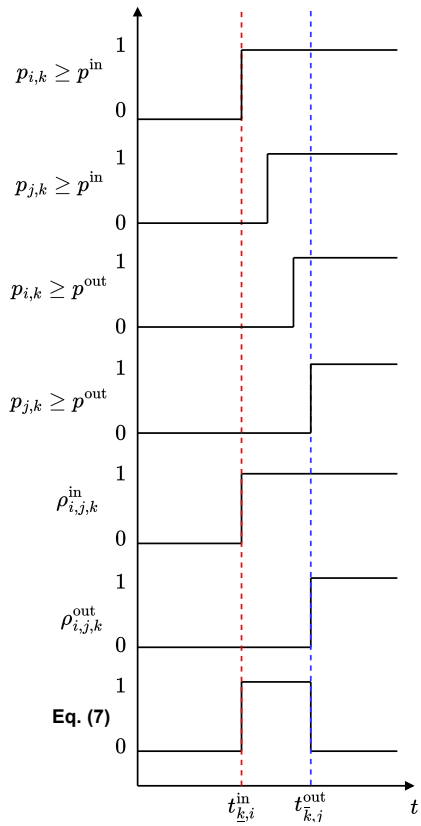

Figure 4.1: Timing diagram of the safety constraint (4.3) activation/deactivation, where the entry condition is based on OR logic of a pair of platoons (i, j) positions w.r.t. CZ, while the exit condition is based on AND.

along with the corresponding conditional constraints of (4.4), (4.5)

$$p_{i,k} - p^{\text{in}} \leq M^{\text{b}} \rho^{\text{in}}_{i,j,k}, \tag{4.7a}$$
$$p_{j,k} - p^{\text{in}} \leq M^{\text{b}} \rho^{\text{in}}_{i,j,k}, \tag{4.7b}$$
$$-2M^{\text{b}}(1 - r_{i,j}) - p_{j,k} + p^{\text{in}} \leq -M^{\text{b}}(\rho^{\text{in}}_{i,j,k} - 1), \tag{4.7c}$$
$$-2M^{\text{b}}(r_{i,j}) - p_{i,k} + p^{\text{in}} \leq -M^{\text{b}}(\rho^{\text{in}}_{i,j,k} - 1), \tag{4.7d}$$
$$-2M^{\text{b}}(r_{i,j}) + p_{j,k} - p^{\text{out}} \leq M^{\text{b}} \rho^{\text{out}}_{i,j,k}, \tag{4.7e}$$
$$-2M^{\text{b}}(1 - r_{i,j}) + p_{i,k} - p^{\text{out}} \leq M^{\text{b}} \rho^{\text{out}}_{i,j,k}, \tag{4.7f}$$
$$-p_{i,k} + p^{\text{out}} \leq -M^{\text{b}}(\rho^{\text{out}}_{i,j,k} - 1), \tag{4.7g}$$
$$-p_{j,k} + p^{\text{out}} \leq -M^{\text{b}}(\rho^{\text{out}}_{i,j,k} - 1). \tag{4.7h}$$

It can be verified that (4.7a), (4.7b) imply (4.4b), while (4.7c), (4.7d) correspond to (4.4a). Similarly, (4.7g), (4.7h) imply (4.4d), while (4.7g), (4.7h) correspond to (4.4c).

To avoid infeasibility, slack variable $\eta_{i,j,k} \geq 0$ is added to (4.6)

$$M^{\text{b}}(1 - \rho^{\text{out}}_{i,j,k} + \rho^{\text{in}}_{i,j,k} + 1 - r_{i,j}) +$$
$$p_{j,k} - l_{j,k} - p_{i,k} - d^{\min} - \bar{l} + \eta_{i,j,k} \geq 0, \tag{4.8a}$$
$$M^{\text{b}}(1 - \rho^{\text{out}}_{i,j,k} + \rho^{\text{in}}_{i,j,k} + r_{i,j}) +$$
$$p_{i,k} - l_{i,k} - p_{j,k} - d^{\min} - \bar{l} + \eta_{i,j,k} \geq 0. \tag{4.8b}$$

For scenarios against leading or isolated HDVs whose trajectories cannot be controlled, the IM can impose a safety constraint to CAV-led platoon $i \in \mathcal{N}$

$$p_{j,k} \geq p_{i,k} + d^{\min}, \ k \in [\underline{k}_j, \bar{k}_i] \tag{4.9}$$

where j denotes the leading HDV. This can be rewritten with the big-M formulation and slack variables as follows

$$M^{\text{b}}(1 - \rho^{\text{out}}_{i,j,k} + \rho^{\text{in}}_{i,j,k}) + p_{j,k} - p_{i,k} - d^{\min} + \eta_{i,j,k} \geq 0, \tag{4.10}$$

where the values of $\rho^{\text{in}}_{i,j,k}, \rho^{\text{out}}_{i,j,k}$ are determined according to conditions (4.7).

In Paper A, it is assumed that (4.1) is always active beyond the CZ, i.e., $\rho^{\text{in}}_{i,j,k}, \rho^{\text{out}}_{i,j,k}$ are not decision variables here.

Lower-Complexity Conditions: The activation/ deactivation mechanism illustrated in Figure 4.1 can still be realized without (4.7c)-(4.7f). This is because they are used to deactivate constraint (4.8), i.e., by setting $\rho^{\text{in}}_{i,j,k} = 0$ & $\rho^{\text{out}}_{i,j,k} = 1$, which implies less restriction on the solution space and potentially produces solutions with lower costs. Therefore, MIP solvers will try to achieve it without the use of (4.7c)-(4.7f) anyway. This leads to the following simplified conditions

$$p_{i,k} - p^{\text{in}} \leq M^{\text{b}} \rho^{\text{in}}_{i,j,k}, \tag{4.11a}$$
$$p_{j,k} - p^{\text{in}} \leq M^{\text{b}} \rho^{\text{in}}_{i,j,k}, \tag{4.11b}$$
$$-p_{i,k} + p^{\text{out}} \leq -M^{\text{b}} (\rho^{\text{out}}_{i,j,k} - 1), \tag{4.11c}$$
$$-p_{j,k} + p^{\text{out}} \leq -M^{\text{b}} (\rho^{\text{out}}_{i,j,k} - 1), \tag{4.11d}$$
$$\rho^{\text{in}}_{i,j,k} \leq \rho^{\text{in}}_{i,j,k+1}, \tag{4.11e}$$
$$\rho^{\text{out}}_{i,j,k} \leq \rho^{\text{out}}_{i,j,k+1}. \tag{4.11f}$$

Additionally, less complex conditions are introduced (4.11e)-(4.11f) to prevent activation of (4.8), (4.10) at time k before $k+1$ is active by exploiting the fact that $v^{\min} > 0$, i.e., vehicles are closer to the intersection in each time k.

Rear-End Collision Avoidance

Consider platoon i moving behind platoon j within the same direction. To avoid rear-end collisions, the position gap between the two platoons must be no smaller than $d^{\min}$,

$$p_{j,k} - l_{j,k} - p_{i,k} \geq d^{\min}. \tag{4.12}$$

For compactness, we lump the constraints (4.8), (4.10), and (4.7)/(4.11) above in $h^{\text{safe}}(p_{i,k}, p_{j,k}) \leq 0$ and as $h^{\text{pos}}(\rho^{\text{in}}_{i,j,k}, \rho^{\text{out}}_{i,j,k}) \leq 0$, respectively.

4.2 Objective Function

In this thesis, from Paper A to D, different forms of objective functions are utilized. In each equation, they essentially contain trade-off terms where one term aims to minimize CAV states deviation from the references or to maximize the velocity such that traffic delays can be minimized while, in the

other term, the amount of acceleration/deceleration (input) or fuel/energy consumption is to be minimized.

Each type of objective functions will be detailed next.

Velocity-Tracking Objective

This objective is used in Paper A-D. Here, CAV $i \in \mathcal{N}$ follows its reference speed v_i^s while also minimizing its acceleration/deceleration over some *prediction* horizon $N^{\text{pre}} \in \mathbb{N}$ (or $T^{\text{pre}} \in \mathbb{R}_+$) as follows

$$J_i(\mathbf{w}_i) = q^{\text{v}}(v_i^{\text{ref}} - v_{i,k})^2 + \sum_{k=\lfloor \frac{t}{\Delta t} \rfloor}^{N^{\text{pre}}-1} q^{\text{v}}(v_i^{\text{ref}} - v_{i,k})^2 + q^{\text{u}} u_{i,k}^2, \tag{4.13}$$

where q^{v} and q^{u} are constant weights.

Car-Following Objective

In Paper A, the following car-following objective is applied for the priority assignment task between a CAV and a HDV. This objective is applied when CAV i follows The HDV j in a virtual platooning mode, while minimizing the cost associated with the input over N^{pre}

$$J_i(\mathbf{w}_i) = J^{\text{p}}_{i,N^{\text{pre}}} + J^{\text{v}}_{i,N^{\text{pre}}} + \sum_{k=\lfloor \frac{t}{\Delta t} \rfloor}^{N^{\text{pre}}-1} J^{\text{p}}_{i,k} + J^{\text{v}}_{i,k} + J^{\text{u}}_{i,k}, \tag{4.14}$$

where

$$J^{\text{p}}_{i,k} = q^{\text{d}}(d^{\text{ref}} - (p_{j,k} - p_{i,k}))^2, \tag{4.15}$$

$$J^{\text{v}}_{i,k} = q^{\text{v}}(v_{j,k} - v_{i,k})^2, \qquad J^{\text{u}}_{i,k} = q^{\text{u}} u_{i,k}^2, \tag{4.16}$$

and $q^{\text{v}}, q^{\text{d}}, r$ denote the weights and d^{ref} is the reference gap. In (4.14) above, the terms $J^{\text{x}}_{i,k},\ \text{x} \in \{p, v\}$ penalize the deviations of CAV i's position and velocity from the safety distance to HDV j and j's velocity, respectively, while the term $J^{\text{u}}_{i,k}$ penalizes i's control effort.

Economic Objective

In this part, an economic cost function is utilized to minimize a trade-off between energy consumption and travel time of a CAV i. This objective function is particularly applied for the case with nonlinear dynamics model (3.7) as in Paper E.

The energy consumption is obtained as the integral of propulsive power over time

$$J^{\mathrm{Eg}}(x_i(t), u_i(t)) = \int_0^{t^f} P^{\mathrm{Eg}}(x_i(t), u_i(t))\ \mathrm{d}t, \tag{4.17}$$

where

$$P^{\mathrm{Eg}}(x_i(t), u_i(t)) = \frac{\tau_i(t)\omega_i(t)}{\eta^{\mathrm{g}}(\tau_i(t), \omega_i(t))}, \tag{4.18}$$

with $\eta^{\mathrm{g}}(\tau_i(t), \omega_i(t))$ denoting the powertrain efficiency [63].

The discretization of the problem by numerical integration over sampling time Δt yields

$$J^{\mathrm{Eg}}(x_{i,k}, u_{i,k}) = \int_{k\Delta t}^{(k+1)\Delta t} P^{\mathrm{Eg}}(x_i(t), u_i(t))\ \mathrm{d}t. \tag{4.19}$$

The problem of minimizing the travel time can be translated into maximization of the average velocity

$$J^{\mathrm{v}}(x_{i,k}) = \frac{1}{\Delta t} \int_{k\Delta t}^{(k+1)\Delta t} v_i(t)\ \mathrm{d}t. \tag{4.20}$$

Hence, the competing-objective problem of (4.19) and (4.20) reads as

$$J^{\mathrm{Eg,v}}(x_{i,k}, u_{i,k}) = q^{\mathrm{Eg}} J^{\mathrm{Eg}}(x_{i,k}, u_{i,k}) - q^{\mathrm{v}} J^{\mathrm{v}}(x_{i,k}), \tag{4.21}$$

where $q^{\mathrm{Eg}}, q^{\mathrm{v}} > 0$ are the constant weights that represents the trade-off between $J^{\mathrm{Eg}}(x_{i,k}, u_{i,k})$ and $J^{\mathrm{v}}(x_{i,k})$. As discussed in [44], the weight values can be selected such that CAV i reaches a given steady-state velocity v_i^{ref}.

Furthermore, a properly defined terminal cost is required to ensure asymptotic stabilization of a system subject to the economic stage cost (4.21), often requiring a nonzero gradient at steady state [64]. Hence, the following terminal

is adopted

$$V^{\mathrm{f}}(x_{i,N^{\mathrm{pre}}}) = \frac{1}{2} q^{\mathrm{f,q}} (v_i^{\mathrm{ref}} - v_{i,N^{\mathrm{pre}}})^2 + q^{\mathrm{f,l}} v_{i,N^{\mathrm{pre}}}, \tag{4.22}$$

where $q^{\mathrm{f,q}}, q^{\mathrm{f,l}}$ are the constant weights. The complete stage and terminal economic objective function over the horizon N^{pre} is

$$J_i(\mathbf{w}_i) = V^{\mathrm{f}}(x_{i,N^{\mathrm{pre}}}) + \sum_{k=\lfloor \frac{t}{\Delta t} \rfloor}^{N^{\mathrm{pre}}-1} J^{\mathrm{Eg,v}}(x_{i,k}, u_{i,k}), \tag{4.23}$$

where $\mathbf{w}_i = [w_{i,1}, ..., w_{i,k}, ..., w_{i,N^{\mathrm{pre}}}]^\top \in \mathbb{R}^{n^{\mathbf{w}}}$ with $w_{i,k} = [x_{i,k}, u_{i,k}]^\top$.

Slack Penalty

Due to the use of slack variables $\eta_{i,j,k}$ in (4.8) (Paper B-D), a corresponding linear and quadratic penalty objective functions is introduced

$$J^{\mathrm{s}}(\boldsymbol{\eta}_{i,j}) = \sum_{k=\lfloor \frac{t}{\Delta t} \rfloor}^{N^{\mathrm{pre}}-1} q^{\mathrm{s,l}} \eta_{i,j,k} + \sum_{k=\lfloor \frac{t}{\Delta t} \rfloor}^{N^{\mathrm{pre}}-1} q^{\mathrm{s,q}} \eta_{i,j,k}^2, \tag{4.24}$$

where $\boldsymbol{\eta}_{i,j} = [\eta_{i,j,0}, ..., \eta_{i,j,k}, ..., \eta_{i,j,N^{\mathrm{pre}}}]^\top$. $q^{\mathrm{s,l}}, q^{\mathrm{s,q}}$ are constants weights for linear and quadratic terms, respectively. The quadratic term is in principle not needed, but it is added to the cost to introduce some positive curvature that can help the solver converge faster.

4.3 Problem Formulation

Here, we formulate an optimization problem consisting of the aforementioned vehicle model, safety constraints, and objective functions as an optimal control problem. While the MIP formulation here is defined as a benchmark algorithm from the optimality viewpoint, the NLP is utilized as part of the heuristic methods.

MIP problem

The vehicle coordination problem is defined as the following Mixed-Integer Program (MIP) problem

$$\Phi^{\text{MIP}}(\mathbf{v}^{\text{ref}}, \boldsymbol{x}_0, \mathbf{p}^{\text{h}}) = \min_{\boldsymbol{\psi}} \quad \sum_{i}^{N} J_i(\mathbf{w}_i) + \sum_{i=1}^{N-1} \sum_{j=i+1}^{N} J^{\text{s}}(\boldsymbol{\eta}_{i,j}) \tag{4.25a}$$

$$\text{s.t.} \quad x_{i,k+1} = F(x_{i,k}, u_{i,k}), \tag{4.25b}$$

$$x_{i,0} = x_i^0, \tag{4.25c}$$

$$h^{\text{limit}}(x_{i,k}, u_{i,k}) \leq 0 \tag{4.25d}$$

$$h^{\text{safe}}(p_{i,k}, p_{j,k}) \leq 0 \tag{4.25e}$$

$$h^{\text{pos}}(\rho^{\text{in}}_{i,j,k}, \rho^{\text{out}}_{i,j,k}) \leq 0, \tag{4.25f}$$

$$r_{i,j}, \rho^{\text{in}}_{i,j,k}, \rho^{\text{out}}_{i,j,k} \in \{0, 1\} \tag{4.25g}$$

where $\boldsymbol{\psi} = [\mathbf{r}, \boldsymbol{\rho}, \mathbf{w}, \boldsymbol{\eta}]^\top$ are the decision variables. The binaries are collected in $\mathbf{r} = [r_{1,2}, ..., r_{i,j}, ..., r_{N-1,N}]^\top$, $\boldsymbol{\rho}^{\text{in}} = \left[\rho^{\text{in}}_{1,2,0}, ..., \rho^{\text{in}}_{N-1,N,N^{\text{pre}}}\right]^\top$, $\boldsymbol{\rho}^{\text{out}} = \left[\rho^{\text{out}}_{1,2,0}, ..., \rho^{\text{out}}_{N-1,N,N^{\text{pre}}}\right]^\top$, $\boldsymbol{\rho} = \left[(\boldsymbol{\rho}^{\text{in}})^\top, \ (\boldsymbol{\rho}^{\text{out}})^\top\right]^\top$. All CAVs states and control inputs are lumped in $\mathbf{w} = [\mathbf{w}_1, ..., \mathbf{w}_i, ..., \mathbf{w}_N]^\top$, and the slack variable are $\boldsymbol{\eta} = [\boldsymbol{\eta}_{1,2}, ..., \boldsymbol{\eta}_{i,j}, ..., \boldsymbol{\eta}_{N-1,N}]^\top$. Furthermore, $\mathbf{v}^{\text{ref}} = \left[v_1^{\text{ref}}, ..., v_N^{\text{ref}}\right]^\top$ collects the steady-state/reference velocities, $\boldsymbol{x}_0 = [x_{1,0}, ..., x_{N,0}]^\top$ contains CAVs initial states, and $\mathbf{p}^{\text{h}} = \left[\mathbf{p}_{i,0:N^{\text{pre}}}, ..., \mathbf{p}_{M,0:N^{\text{pre}}}\right]^\top$ are the trajectories of HDVs used to define i-th length $l_{i,k}$. The functions $h^{\text{limit}}(x_{i,k}, u_{i,k}), h^{\text{safe}}(p_{i,k}, p_{j,k})$, $h^{\text{pos}}(\rho^{\text{in}}_{i,j,k}, \rho^{\text{out}}_{i,j,k})$ collect the vehicle limitations (3.5)/(3.11), collision avoidance (4.8), (4.12), and activation/deactivation constraints (4.7)/(4.11), respectively.

Depending on the vehicle model, implementation of (4.1), and objective functions, MIP (4.25) can be denoted as Mixed-Integer Quadratic Program (MIQP)(Paper B & C) or Mixed-Integer Non Linear Program (MINLP) (Paper A & D). By solving the MIP and examining $\mathbf{r}$, the CAV-led platoons intersection *crossing order* $\mathcal{O}_k = [o_{1,k}, ..., o_{\upsilon,k}, ..., o_{N,k}]^\top$ can be defined, in which $o_{\upsilon,k} = i$ entails that platoon i crosses the intersection in sequence υ.

CAV-HDV prioritization: In Paper A, a pair of CAV and HDV priority assignment problem is addressed. In this problem, the following switching be-

tween the car-following (4.14) and velocity-tracking(4.13) objectives is implemented within formulation (4.25) as MINLP

$$J_i(\mathbf{w}_i) = \begin{cases} \text{Eq. (4.14)} & \text{if} \quad \mathcal{P}_k == 0 \quad \text{(4.26a)} \\ \text{Eq. (4.13)} & \text{else if} \quad \mathcal{P}_k == 1. \quad \text{(4.26b)} \end{cases}$$

Objective (4.26a) is used when the priority (order) $\mathcal{P}_k = 0$, i.e., CAV i follows HDV j, whereas (4.26b) ($\mathcal{P}_k = 1$) is applied when i virtually overtakes j and thus, the collision avoidance constraint is no longer used.

MIP problem (4.25) can be executed in a closed-loop fashion. Before a platoon reaches the CZ, the problem is solved to determine $\mathbf{r}$, i.e., $\mathcal{O}_k$, $\boldsymbol{\rho}$, and CAVs control actions. Once a platoon is close to CZ, $\mathcal{O}_k$ is fixed and a fixed-binaries Nonlinear Program (NLP) problem (4.27) is solved instead to update the CAVs control actions.

NLP problem

In the case where the binaries $\mathbf{r}$, $\boldsymbol{\rho}$ containing the crossing order $\mathcal{O}_k$ are known (given), we can redefine the non-smooth MIP (4.25) above as the following continuous, fixed-binaries Non Linear Program (NLP)

$$\begin{aligned} \Phi^{\text{NLP}}(\boldsymbol{x}^{\text{p}}) = \min_{\mathbf{w},\boldsymbol{\eta}} \quad & \sum_{i}^{N} J_i(\mathbf{w}_i) + \sum_{i=1}^{N-1} \sum_{j=i+1}^{N} J^{\text{s}}(\boldsymbol{\eta}_{i,j}) && \text{(4.27a)} \\ \text{s.t.} \quad & x_{i,k+1} = F(x_{i,k}, u_{i,k}), && \text{(4.27b)} \\ & x_{i,0} = x_i^0, && \text{(4.27c)} \\ & h^{\text{limit}}(x_{i,k}, u_{i,k}) \leq 0, && \text{(4.27d)} \\ & h^{\text{safe}}(p_{i,k}, p_{j,k}) \leq 0, && \text{(4.27e)} \end{aligned}$$

where $\boldsymbol{x}^{\text{p}} = [\mathbf{v}^{\text{ref}}, \boldsymbol{x}_0, \mathbf{p}^{\text{h}}, \mathbf{r}, \hat{\boldsymbol{\rho}}]^\top$ lumps the parameters and $\boldsymbol{\vartheta} = [\mathbf{w}, \boldsymbol{\eta}]^\top$. If (4.25) is instead MIQP, as in Paper B & C, then (4.27) here is simply Quadratic Programming (QP). In Paper A, each choice of priority $\mathcal{P}_k$ also has its own QP (4.27).

4.4 Heuristic Methods

It is known that solving MIP (4.25) using *off-the-shelves* MIP solvers in a closed-loop manner for large-sized problem is not a computationally viable option due to the use of binaries $\mathbf{r}, \boldsymbol{\rho}$ as decision variables. Hence, heuristics methods to alternatively retrieve approximately optimal initial solutions and address reordering scenarios are presented here.

Initial Solutions

As mentioned in Chapter 1, we present heuristic methods to solve the initial crossing order problem. In Paper B, a feasibility-enforcing Alternating Direction Methods of Multipliers (ADMM) is proposed, which is intended to obtain the approximate initial solution for MIQP (4.25) formulated in Paper C. For Paper D, the initial solution can obtained via *off-the-shelves* MINLP solver, FCFS, or ADMM. For Paper A, the priority is initially set to $\mathcal{P}_k = 0$.

The feasibility-enforcing ADMM is utilized to obtain the binaries $\mathbf{r}$, $\boldsymbol{\rho}$ by approximately solving MIQP (4.25). The approach here makes use of the ADMM from [29] but is paired with feasibility checking and enforcing functions tailored to the coordination problem (4.25) to improve the quality of solutions. The details of the ADMM here are explained next.

Augmented Lagrangian form: To use ADMM, an Augmented Lagrangian (AL) form of (4.25) is required. In AL, the coupling inequalities (4.25e) - (4.25f) are turned into equalities [65] by adding dummy variables $\boldsymbol{b} = [b^{\mathrm{s}}, b^{\rho}]^{\top} \in \mathbb{R}_{>0}$. Hence, MIQP (4.25) is rewritten as

$$
\begin{aligned}
\Phi^{\mathrm{MIQP}}(\mathbf{v}^{\mathrm{ref}}, \boldsymbol{x}_0, \mathbf{p}^{\mathrm{h}}) = \min_{\boldsymbol{\psi}} \quad & \sum_{i}^{N} J_i(\mathbf{w}_i) + \sum_{i=1}^{N-1} \sum_{j=i+1}^{N} J^{\mathrm{e}}(\boldsymbol{\eta}_{i,j}) \\
& + I(\mathbf{w}_i) + I(\boldsymbol{\eta}_{i,j}) + I(\mathbf{r}) + I(\boldsymbol{\rho}) && \text{(4.28a)} \\
\text{s.t.} \quad & x_{i,k+1} = Ax_{i,k} + Bu_{i,k}, && \text{(4.28b)} \\
& x_{i,0} = x_i^0, && \text{(4.28c)} \\
& h^{\mathrm{safe}}(p_{i,k}, p_{j,k}) + b^{\mathrm{s}} = 0, && \text{(4.28d)} \\
& h^{\mathrm{pos}}(\rho_{i,j,k}^{\mathrm{in}}, \rho_{i,j,k}^{\mathrm{out}}) + b^{\rho} = 0, && \text{(4.28e)}
\end{aligned}
$$

where the indicator functions $I(\mathbf{w}_i), I(\boldsymbol{\eta}), I(\mathbf{r}), I(\boldsymbol{\rho})$ represent the box (non-coupled) constraints of (4.25d), (4.25g). The augmented Lagrangian form of (4.28) is written as

$$\begin{aligned}\mathcal{L}(\boldsymbol{\psi},\boldsymbol{b}) = &\sum_{i}^{N} J_i(\mathbf{w}_i) + \sum_{i=1}^{N-1}\sum_{j=i+1}^{N} J^{\mathrm{e}}(\boldsymbol{\eta}_{i,j}) + \\ &I(\mathbf{w}_i) + I(\boldsymbol{\eta}_{i,j}) + I(\mathbf{r}) + I(\boldsymbol{\rho}) + \\ &\frac{\nu_1}{2}||Ax_{i,k} + Bu_{i,k} - x_{i,k+1} + \lambda_1||^2 + \\ &\frac{\nu_2}{2}||x_{i,0} - x_i^0 + \lambda_2||^2 + \frac{\nu_3}{2}||h^{\mathrm{safe}} + b^{\mathrm{s}} + \lambda_3||^2 + \\ &\frac{\nu_4}{2}||h^{\mathrm{pos}} + b^{\rho} + \lambda_4||^2,\end{aligned} \tag{4.29}$$

where the ν_{1-4} are the weights and $\boldsymbol{\lambda} = \lambda_{1-4}$ are their associated dual variables. This AL is solved using ADMM iterations explained next.

ADMM iterations: The ADMM algorithm consists of L^{out} outer and L^{in} inner iterations. In each inner iteration n, the following set of primal and dual equations is computed

$$\begin{bmatrix}\boldsymbol{\psi}^{n+1/2} \\ \boldsymbol{b}^{n+1/2}\end{bmatrix} = \arg\min \mathcal{L}(\boldsymbol{\psi}^n, \boldsymbol{b}^n), \tag{4.30a}$$

$$\begin{bmatrix}\boldsymbol{\psi}^{n+1} \\ \boldsymbol{b}^{n+1}\end{bmatrix} = \boldsymbol{\Pi}\left(\begin{bmatrix}\boldsymbol{\psi}^{n+1/2} \\ \boldsymbol{b}^{n+1/2}\end{bmatrix} + \begin{bmatrix}0 & I\end{bmatrix}\boldsymbol{\lambda}^n\right), \tag{4.30b}$$

$$\lambda_1^{n+1} = \lambda_1^n + Ax_{i,k} + Bu_{i,k} - x_{i,k+1}, \tag{4.30c}$$

$$\lambda_2^{n+1} = \lambda_2^n + x_{i,0} - x_i^0, \tag{4.30d}$$

$$\lambda_3^{n+1} = \lambda_3^n + h^{\mathrm{safe}} + b^{\mathrm{s}}, \tag{4.30e}$$

$$\lambda_4^{n+1} = \lambda_4^n + h^{\mathrm{pos}} + b^{\rho}, \tag{4.30f}$$

where $\boldsymbol{\Pi}$ is a projection function. Additionally, the primal and dual variables are initialized with randomized values within the bounds.

Next, $f^{\mathrm{viol}}(\boldsymbol{\psi}^n)$ is applied to count violations occurring in (4.25e) w.r.t. $\mathcal{O}_k^n$. This function is implemented alongside the norm of equalities $g(\boldsymbol{\psi}^n)$ that contains (4.28b), (4.28c). This combination aims to eliminate solutions that have an unfavorable order $\mathcal{O}_k$ typically associated with a higher input cost

and infeasible activation binaries $\boldsymbol{\rho}$. Finally, the best approximated solution $\hat{\boldsymbol{\psi}}^*$ is retained based on cost merit, i.e., $\mathbf{J}(\boldsymbol{\psi}^n)$ of (4.28a).

Feasibility check: When solving the problem (4.29), ADMM solutions may yield infeasible $\mathcal{O}_k$ and fail to satisfy (4.25e). Therefore, a set of problem-tailored feasibility check functions is applied within and at the end of ADMM iterations.

The first function is to check whether the combination of $\mathbf{r}^n$ leads to a feasible $\mathcal{O}_k$. If it is infeasible, $\mathbf{r}^n$ is replaced by binaries obtained from, e.g., First-Come, First-Serve (FCFS). The second function is to evaluate whether $\boldsymbol{\rho}^n$ fulfills (4.11e), (4.11f).

Finally, the third function, executed after ADMM iterations are done, involves solving the following fixed-binaries QP (4.27) to retain feasible trajectories involving the continuous variables $\mathbf{w}, \boldsymbol{\eta}$ w.r.t. the resulting binaries $\hat{\mathbf{r}}^*$, $\hat{\boldsymbol{\rho}}^*$ extracted from $\hat{\boldsymbol{\psi}}^*$. The resulting control inputs are then applied to the CAVs.

Reordering Scenarios

As fixing crossing order $\mathcal{O}_k$ in closed-loop applications, i.e., at time $t_k > 0$, might not be reasonable, the *change of order* (reordering) is required. In particular, if the current $\mathcal{O}_k$ is either leading to a potential accident or is no longer beneficial, a safe and more efficient trajectories can be obtained by selecting a different order. As solving MIP (4.25) in closed-loop setting is not tractable, heuristic methods are proposed here.

The reordering problem is first investigated in Paper A with a simple, low-complexity setting: a pair of vehicles (a CAV and a HDV) approaching an intersection as illustrated in Figure 4.2. Additionally, the use of sensitivity information to approximate the cost function is studied. Next, the investigation continues to the multi-vehicle coordination setting of CAVs and HDVs, as illustrated in Figure 3.1 in Chapter 3. This larger setting are discussed in Paper C and D. The summary of the proposed heuristics in those three papers are provided next.

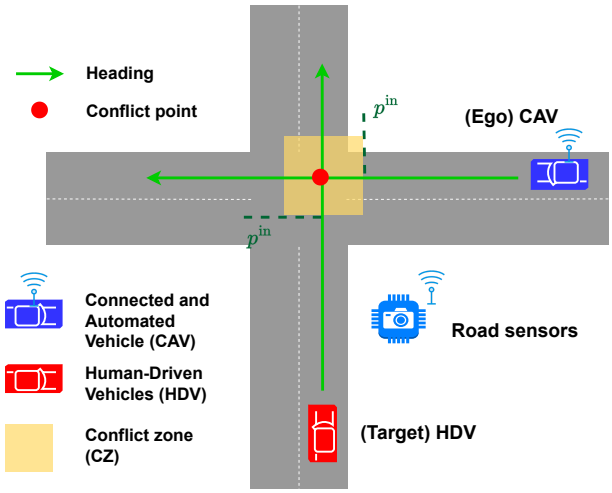

Figure 4.2: A Pair of CAV and HDV at an unsignalized intersection

CAV-HDV Sensitivity-based Re-prioritization

As mentioned above, the task of the heuristic presented in Paper A is to decide the priority $\mathcal{P}_k$ at time k depending on the vehicles states and parameter $\boldsymbol{x}^{\text{p}}$. The idea underlying the heuristic here is to switch $\mathcal{P}_k$ in the case where the HDV j behavior is leading to an increase of the cost beyond a prescribed bound.

Given that the initial $\mathcal{P}_k = 0$ and a corresponding QP is solved, solution $\mathrm{w}_i^*(\tilde{\mathbf{x}}^{\text{p}})$ and its sensitivities are retrieved. For the next time steps $k > 0$, the cost (4.14) can be approximated using (2.10). In this way, the cost can be monitored in order to detect its growth beyond the following bounds

$$J_i(\hat{\mathbf{w}}_i^*(\boldsymbol{x}^{\text{p}})) \leq J^{\text{ub}}, \ \forall k \in \{0, N^{\text{pre}}\}, \tag{4.31}$$

where J^{ub} contains the constants that represent the maximum allowed gap, velocity tracking error from HDV j, and CAV i's braking efforts.

If any violation is detected in (4.31) for $n^{\max}$ consecutive times, then the priority is switched to $\mathcal{P}_k = 1$.

Multi-Vehicle Coordination: Exact Heuristic (EH)

The heuristic for multi-vehicle settings here exploits the nature of the vehicle coordination problem formulated in MIP (4.25). The framework mainly consists of two modules: *feasibility-based consistency check* and NLPs/QPs *cost comparison*. Both modules are executed in the closed-loop setting. As the NLPs/QPs are solved in the *exact* way, the framework here is denoted as Exact Heuristic (EH).

Consistency Check (Clustering) A reordering is potentially required when the position gap between a pair of adjacent-sequence platoons in $\mathcal{O}_k$ becomes smaller and may violate collision avoidance constraint (4.27e). Thus, an attempt to reduce the complexity of (4.25) can be made by clustering and targeting a smaller subset of pairs of interests, as well as preventing *false positive* trigger. To that end, the following steps are taken:

Step 1: At each time step $k > 0$, we check the predicted (4.27e) over N^{pre} w.r.t. $\mathcal{O}_{k-1}$ for each pair of platoons (i, j). In particular, this check is applied to any pair whose *preceding* one j (currently) is a non-isolated platoon. This is because j contains HDV(s) which may change their trajectories. Hence, j and its immediate following platoon i are collected in the set $\mathcal{N}_k^{\text{T}}$. The pair (i, j) is excluded if they come from the same direction.

For a pair $(i, j) \in \mathcal{N}_k^{\text{T}}$, we check the feasibility of the stacked vector

$$h^{\text{safe}}(p_{i,k}, p_{j,k}) \leq 0,\ k \in [k-1, k-1+N^{\text{pre}}] \tag{4.32}$$

where $p_{i,k}, p_{j,k}$ are extracted from solution $\mathbf{w}$ of (4.27) at $k-1$.

Step 2: A violation occurs if any of the rows of $h_i^{\text{safe,check}} > 0$. This event is recorded in s_i. When the violation occurs for some consecutive times, i.e., $s_i = n^{\max}$, the pair (i, j) is added to the set $\mathcal{E}_k$.

Cost comparison To decide which order $\mathcal{O}_k$ to select (the current one or the one swapping the order of one or more pairs of platoons $i, j \in \mathcal{E}_k$), we compare their respective costs by solving the associated *fixed-binaries* NLPs (Paper D) or they are instead QPs (Paper C).

For each pair (i, j), two NLPs (4.27) are constructed, namely Problem A $\Phi_{i|j}^{\text{NLP}}$ (current order) and Problem B $\Phi_{j|i}^{\text{NLP}}$ (alternative). The difference between them is the crossing order of i and j, which is reversed in the alterna-

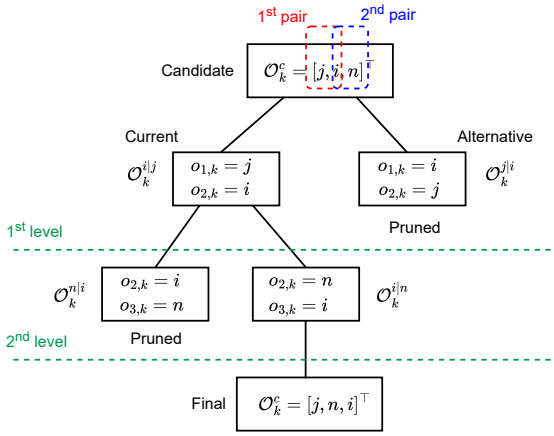

Figure 4.3: Tree structure for sequential cost comparison

tive order, denoted as , i.e., $\mathbf{r}^{i|j} = [r_{1,2}, ..., 0, ..., r_{N-1,N}]^\top$ (for Problem A) and , i.e., $\mathbf{r}^{j|i} = [r_{1,2}, ..., 1, ..., r_{N-1,N}]^\top$ (for Problem B), respectively. The other components of $\boldsymbol{x}^{\mathrm{p}}$ are the same for the two NLPs. Integers $\hat{\boldsymbol{\rho}}$ are obtained from the previous solution $\mathbf{w}$ at time $k-1$.

To select the best order among the two, both NLPs are solved and their cost is compared. The order associated with the lowest cost is then selected. This comparison process over an entire simulation is illustrated in Figure 4.4a, where the order is switched at $t_k = 1.5$ s when the cost of $\Phi_{i|j}^{\mathrm{NLP}}$ starts to get higher than the alternative sequence.

For *multiple* alternative orders resulting from multiple pairs in $\mathcal{E}_k$, a tree [53] tailored to the coordination problem here is organized as depicted in Figure (4.3). In the figure, the comparison process starts sequentially from the first pair (j, i) to the latest pair (i, n) in $\mathcal{E}_k$. During the process, the candidate order $\mathcal{O}_k^{\mathrm{c}}$ is initialized and updated at each level according to the cost comparison result. The new order $\mathcal{O}_k$ is eventually taken from the last $\mathcal{O}_k^{\mathrm{c}}$. Afterward, the associated control inputs can be implemented in the CAVs. If any platoon reaches p^{in}, $\mathcal{O}_k$ is fixed.

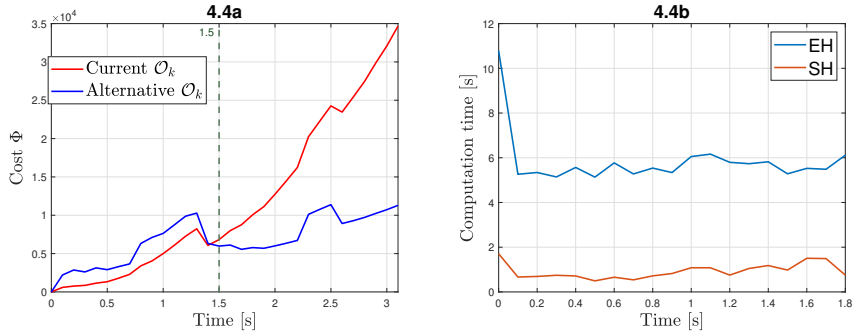

Figure 4.4: Illustration of cost comparison between current and alternative costs (4.4a) and computation time for a closed-loop simulation comparison between EH and SH (4.4b).

Multi-Vehicle Coordination: Sensitivity-based Heuristic (SH)

In the EH framework above, solving multiple NLPs (4.27) (Paper D) associated with current and alternative orders in an *exact* way can be more time-consuming. Thus, a computationally cheaper strategy is proposed by deploying parametric sensitivity-based local quadratic approximation tools as described in Chapter 2 denoted SH.

SH inherits essentially a framework similar to that of EH, including the consistency check and cost comparison modules. Their difference lies in the approximation of NLPs' solutions of the current and alternative orders (instead of exactly solving them) and the additional sensitivities computation of the NLP instances.

The sensitivity computation in SH is summarized as follows: after the initial $\mathcal{O}_k$ is retrieved or anytime reordering occurs, the sensitivities of the NLPs (4.27) of the current and alternative orders are (re-)computed. This requires solving the NLPs with the current (nominal) parameter $\tilde{\boldsymbol{x}}^{\mathrm{p}}$ to obtain the nominal solution $\tilde{\boldsymbol{\vartheta}}$ at some k. Henceforth, when the cost comparison is triggered in the future steps $k+1, k+2, ...$, the cost (4.27a) of the NLP instances can be retrieved using the approximated $\hat{\boldsymbol{\vartheta}}$ via the predictor-corrector QP (2.12) w.r.t. future parameter $\boldsymbol{x}^{\mathrm{p}}$. The comparison of computation times (in seconds) in a closed-loop simulation between EH and SH is depicted in Figure (4.4)b, where it can be observed that SH outperforms EH at all times.

CHAPTER 5

Numerical results

In this chapter, selected numerical results from the appended papers are presented and discussed to evaluate the proposed heuristics against the benchmark MIP and other heuristics. All results are generated using MATLAB simulations with CasADi framework. Bonmin [66] is used to solve MIP problems, whereas QP/NLP is solved via IPOPT [67].

The setting here involves a fixed number of $\mathcal{N}$ CAVs and $\mathcal{M}$ HDVs approaching a symmetric, unsignalized four-junction where the CZ is located in the middle as depicted in Figure 5.1. The discussion on the simulation results are detailed next.

5.1 Alternative heuristics

For comparison, alternative heuristics are used here: First-Come, First-Serve (FCFS) [23] and the Time-To-Intersection (TTI) heuristic [40]. FCFS is obtained by sorting the platoons priority based on the order of entering the intersection area, which translates to $\mathcal{O}_k$. TTI sorts the platoons by their

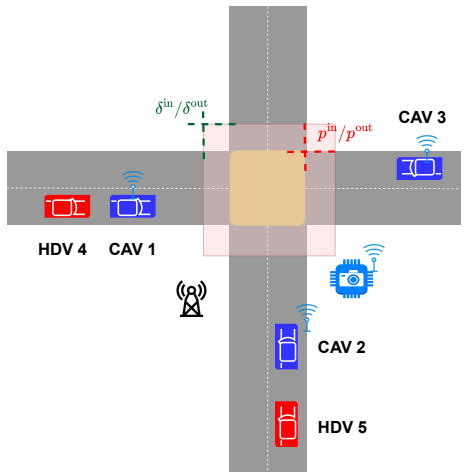

Figure 5.1: Vehicles configuration for simulations.

estimated time to reach the intersection entry, defined as

$$t_{i,k}^{\text{TTI}} = \frac{p^{\text{in}} - p_{i,k}}{v_{i,k}}. \tag{5.1}$$

The platoon with the shortest $t_{i,k}^{\text{TTI}}$ is put first in $\mathcal{O}_k$. Both methods are essentially similar except that, while TTI continuously updates $\mathcal{O}_k$, FCFS keeps it fixed instead. For both methods, at time $k = 0$, the binaries $\mathbf{r}$ are computed by solving (4.27) without enforcing safety constraint (4.1). For $k > 0$, variables $\mathbf{r}$ are obtained from the previously computed trajectories.

5.2 Performance metrics

For performance evaluation, the following metrics are considered.

- *Crossing order and reordering* ($|\tau|$): the evolution of $\mathcal{O}_k$ and the number of occasions (cardinality) in which the crossing order is changed, i.e., $\mathcal{O}_k \neq \mathcal{O}_{k-1}$ from each method.

- *Total and average closed-loop cost* ($\Phi^{\text{cl}}/\Phi^{\text{avg,cl}}$): the total (and average) closed-loop objective values (cost) from all CAVs over the simulation duration T^{sim} s (N^{sim} steps).
- *Average braking energy consumption* ($\mathbf{E}^{\text{avg,Eg}}$): the average braking energy consumed by a CAV at a timestep k.
- *Average of velocity* ($\mathbf{v}^{\text{avg}}$): the average velocity of a CAV.
- *Maximum computation time/timestep* ($\mathbf{t}^{\text{min/max}}$): the worst-case computation times required for solving the crossing order problem at a single time k.

5.3 Results Evaluation

Collision Avoidance and Reordering

In Paper B, the proposed ADMM is tested against MIQP (4.25) with simplified conditions (4.11), i.e., SMIQP, solved via Bonmin as the optimal benchmark. Both methods are executed in closed-loop. The simulations result for $\mathcal{N} = 3, \mathcal{M} = 2$ is presented in Figure 5.2. In Figure 5.2a, it can be observed that the MIQP curves (dashed) coincide closely with ADMM (solid). Both approaches manage to safely avoid any lateral collision by properly maintaining the minimum gap $d^{\min}$ inside the CZ between the incoming vehicles, as indicated by the dashed and solid dark brown vertical lines. Also, the vehicles from both approaches access the CZ using the same $\mathcal{O}_k$.

From Figure 5.2b, ADMM manages to avoid constraint (4.6) violation by accelerating platoon 3 (CAV 3) and braking platoon 1 (CAV 1 and HDV 4) and platoon 2 (CAV 2 and HDV 5). The trajectories of ADMM are slightly seen to be different from those of MIQP. The rest of the curves are similar. In terms of cost, MIQP is $\Phi^{\text{cl}} = 6126.93$, whereas ADMM is $\Phi^{\text{cl}} = 6353.22$. This shows the capability of ADMM to yield close-to-optimal solutions. In terms of $\mathbf{t}^{\max}$, ADMM is 22 times faster than MIQP in terms of $\mathbf{t}^{\max}$.

In Paper C, the proposed Exact-Heuristic (EH) reordering algorithm is compared with MIQP (4.25), FCFS, and TTI. Here, an experiment with reordering scenario with similar setting as in Figure 5.1 above, but all CAV-led platoons must additionally yield to the isolated HDV 6 that comes from the north.

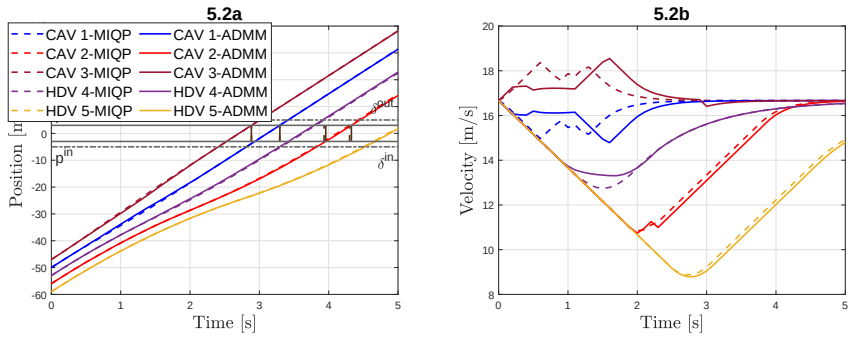

Figure 5.2: Position/trajectory (Figure 2a), velocity ((Figure 2b), and crossing order (Figure 2c) profiles from MIQP (dashed lines) and ADMM (solid lines). The vertical dark brown dashed line indicates $d^{\min}$. In Figure 2c, the colors on the lines indicate the sequence within $\mathcal{O}_k$.

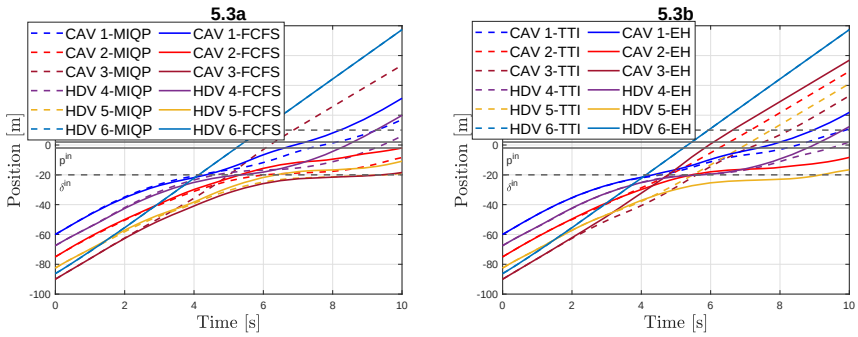

Figure 5.3: Position trajectories $p_{i,k}$ of all vehicles (CAVs and HDVs) approaching the intersection's CZ from MIQP and FCFS (Figure 5.2a), TTI and EH (Figure 5.2b).

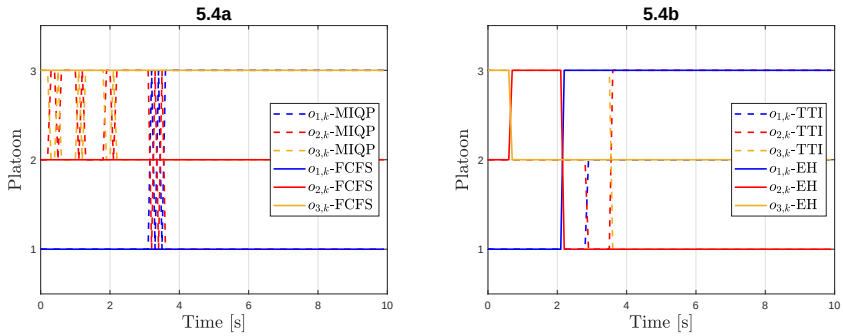

Figure 5.4: Crossing order $\mathcal{O}_k$ of MIQP and FCFS (Figures 5.3a), TTI and EH (Figure 5.3b). The line colors represent the index inside $\mathcal{O}_k$, e.g., blue is the first, i.e., $o_{1,k}$ and so on.

In Figure 5.3, it can be observed that all CAV-led platoons from all methods initially move according to the crossing order dictated by their initial positions, i.e., $\mathcal{O}_{k=0} = [1, 2, 3]^\top$. Due to the use of safety constraint (4.10) against HDV 6, the CAV-led platoons need to decelerate, except for platoon (CAV) 3 which leads to reordering events. Reordering is not the case for FCFS that fixes its order, as can be confirmed in Figure 5.4a.

In MIQP, TTI, and EH, as platoons 1 and 2 slow down, the tail HDVs behind them are forced to decelerate. This action is necessary to maintain safety at CZ. In Figure 5.4a, it can be observed that MIQP suffers from order chattering with $|\boldsymbol{\tau}| = 14$, whereas EH and TTI require only a single order swap in each reordering, i.e., $|\boldsymbol{\tau}| = 2$. In Figure 5.4b, it can be seen that EH can converge to the same final order $\mathcal{O}_k = [3, 1, 2]^\top$ as MIQP, whereas TTI has different order $\mathcal{O}_k = [2, 3, 1]^\top$. In terms of cost, MIQP is $\Phi^{\text{cl}} = 160883.32$, FCFS is $\Phi^{\text{cl}} = 202020.83$, TTI is $\Phi^{\text{cl}} = 407715.49$, and EH is $\Phi^{\text{cl}} = 157617.62$.

The result of this experiment shows that EH can yield solution close to MIQP in reordering scenarios and outperform FCFS and TTI, while being 280 times faster than MIQP in terms of $\mathbf{t}^{\max}$.

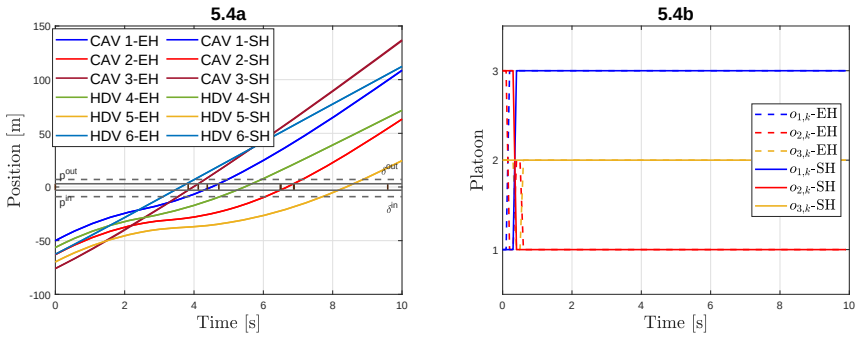

Figure 5.5: Position trajectories $p_{i,k}$ of all vehicles (Figure 5.2a) and crossing order $\mathcal{O}_k$ (Figure 5.2b) of EH and SH in *medium* CAVs traffic penetration.

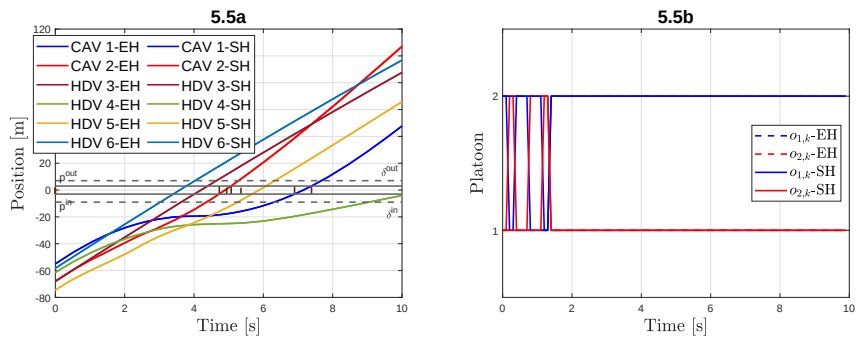

Figure 5.6: Position trajectories $p_{i,k}$ of all vehicles (Figure 5.2a) and crossing order $\mathcal{O}_k$ (Figure 5.2b) of EH and SH in *low* CAVs traffic penetration.

Table 5.1: Average performance comparison for a CAV i at a timestep k

Experiment	Methods	$\Phi^{\text{avg,cl}}$	$\mathbf{E}^{\text{avg,Eb}}$ [J]	$\mathbf{v}^{\text{avg}}$ [m/s]
High	FCFS	-1.27	1768.91	16.42
	EH	-1.34	1535.87	17.59
	SH	-1.34	1535.87	17.59
Medium	FCFS	-0.92	2124.87	12.31
	EH	-1.30	1541.54	16.24
	SH	-1.30	1539.15	16.59
Low	FCFS	-0.83	2840.74	10.50
	EH	-0.92	2306.76	13.93
	SH	-0.92	2306.60	13.95

Experiments with Different CAVs Penetrations

In this part, the performance of SH is compared against EH and FCFS for the economic optimal coordination task in a different mixed traffic setting, as covered in Paper D. Hence, the following results from experiments with *high*, *medium*, and *low* CAVs penetration rates are presented.

In each experiment, 10 simulations are carried out, each with various initial positions of the HDVs. The result is then averaged and presented in Table 5.1. In Figure 5.5, the position trajectories and the crossing order of one of the simulations in the medium penetration are presented. Here, several reorderings are performed by the platoons to maximize v^{avg} and thus minimize braking energy $\mathbf{E}^{\text{avg,Eb}}$. It is interesting to see that both methods generate approximately the same trajectories. The slight difference between EH and SH is illustrated in the reordering evolution seen in Figure 5.5b where their reordering patterns are slightly different, where EH suffers from a few chatterings. However, this does not significantly affect the solution. Additionally, SH is around $4-10$ times faster than EH. In the low penetration experiment, it can be seen in Figure 5.6b that when the CAVs need to accommodate the behavior of the increasing number of HDVs, the chatter can be worse.

The performance degradation is seen in Table 5.1, where we can see that as the CAVs penetration is reduced, the average cost $\Phi^{\text{avg,cl}}$ and energy $\mathbf{E}^{\text{avg,Eb}}$ increase whereas the velocity v^{avg} decreases. This shows that CAVs pene-

tration rate can play important role to improve economical aspects of traffic coordination. Also, the average cost $\Phi^{\text{avg,cl}}$ of EH & SH are better than that of the fixed-order FCFS.

5.4 Summary

In this chapter, the selected results demonstrate that the proposed ADMM, EH, and SH perform remarkably well in terms of optimality, computational, and economical aspects. The ADMM can approximately solve the MIQP (4.25) multiple times faster than the off-the-shelves MIP solver, while attaining near-optimal solutions (Paper B). A similar notion is seen in EH where it can be few hundreds times faster than MIP and obtain reasonably good solutions which are better than the alternative heuristics (Paper B). Furthermore, SH accelerates the NLPs approximate solving process within the heuristic such that the cost comparison can be performed faster (Paper D).

In different CAV penetration experiments (Paper D), it can be seen that reducing the ratio of CAVs against HDVs indeed degrades the traffic performance from both traffic and energy viewpoints, as CAV needs to adapt more to HDVs trajectories.

CHAPTER 6

Summary of included papers

This chapter provides a summary of the included papers and individual contributions.

6.1 Paper A

Muhammad Faris, Paolo Falcone, Mario Zanon
A Sensitivity-Based Heuristic for Vehicle Priority Assignment at Intersections
Published in IFAC World Congress,
pp. 4922–4928, Jul. 2023.
 DOI: 10.1016/j.ifacol.2023.10.1265 .

This paper discusses the possibility of exploiting the sensitivity analysis tools to retain approximate solutions to the vehicle reordering problem and we can develop a heuristic approach accordingly. We provide an instance of a two-vehicle priority assignment, an ego CAV, and a target HDV approaching an intersection, which is formulated as MINLP problem, with switching costs and constraint sets w.r.t. to the selected order between those vehicles.

The heuristic relies on the first-order Taylor formula used to approximate the solution given the HDV trajectories prediction and the nominal solution at the initial time. The sensitivities are factorized from the KKT matrix under continuity assumptions. In closed-loop simulations, we construct the approximated cost that we evaluate against some bounds, i.e., we monitor the cost's growth and the order is switched if it is beyond the bounds. We show in simulations that the sensitivity-based heuristic can work faster than MINLP while it is more optimal than FCFS, i.e., the change of order (reordering) timing is on average close to the one from MINLP.

Individual contributions from each author are listed as follows:

- **Muhammad Faris** worked on the ideas, methodology, programming, and manuscript writing.
- **Paolo Falcone** was involved in the ideas discussions, methodology, supervision, manuscript review and editing, and managed project funding.
- **Mario Zanon** worked on the methodology, supervision, and manuscript review.

6.2 Paper B

Muhammad Faris, Mario Zanon, Paolo Falcone
CAVs Coordination at Intersections in Mixed Traffic Via Feasibility-Enforcing ADMM
Published in IEEE International Conference on Intelligent Transportation Systems (ITSC),
pp. 882-888, Sep. 2024.
 DOI: 10.1109/ITSC58415.2024.10919611 .

This paper treats the problem of efficiently approximating MIQP solution of platooning-based coordination, mainly to obtain initial crossing order and safety constraint activation binaries by using an ADMM technique paired with problem feasibility check. The MIQP problem consists of vehicle model, limitation, longitudinal and lateral safety constraint, and reference speed tracking objective function. As solving MIQP is not tractable, ADMM is alternatively deployed. To that end, AL form is formulated with some indicator functions. The ADMM consists of an inner and outer loops, where in the former, the

primal and dual solutions are updated by solving the AL and in the latter, the variables are randomly initialized. To ensure the solutions within the inner iterations are feasible w.r.t. the platooning coordination, check functions are used to evaluate whether the binaries associated with crossing order can yield feasible sequence and the safety constraint is correctly activated. The simulation results over different scenarios show that the ADMM can produce close-to-optimal solutions while being faster dozen times than the MIQP solver.

Individual contributions from each author are listed as follows:

- **Muhammad Faris** worked on the ideas, methodology, programming, and manuscript writing.
- **Mario Zanon** worked on the ideas, methodology, supervision, and manuscript review and editing.
- **Paolo Falcone** was involved in the discussions on the ideas, supervision, manuscript review and editing, and managed project funding.

6.3 Paper C

Muhammad Faris, Mario Zanon, Paolo Falcone
An Optimization-based Dynamic Reordering Heuristic for Coordination of Vehicles in Mixed Traffic Intersections
Published in IEEE Transactions on Control Systems Technology, pp. 1-16, December 2024.
 DOI: 10.1109/TCST.2024.3508542 .

This paper addresses the dynamic coordination problem of CAVs in mixed traffic at unsignalized intersections. Specifically, the reordering issues with multiple CAVs and HDVs in platooning schemes are considered here. As repeatedly solving MIQP in a closed-loop fashion is deemed intractable, a computationally efficient heuristic algorithm is developed instead. The work begins by formulating the platooning-based coordination problem, which yields original MIQP (OMIQP) and simplified MIQP (SMIQP) problems, in which the latter has lower complexity. As exactly solving MIQP in closed-loop is not tractable, a heuristic algorithm is proposed. The heuristic overcomes this challenge by combining a constraint violation/consistency check and QPs cost

comparison. The consistency check is used to restrict reordering actions to a smaller subset of platoons, therefore mitigating subproblems branching complexity. Next, the cost comparison decides whether an order change takes place or not by comparing the cost of the current and alternative orders. In simulations, it is shown that the heuristic can be hundreds of times faster than the OMIQP and SMIQP while minimizing chattering issues and retaining close-to-optimal solutions w.r.t. the benchmark MIQPs and can be better than TTI and FCFS.

Individual contributions from each author are listed as follows:

- **Muhammad Faris** worked on the ideas, methodology, programming, and manuscript writing.
- **Mario Zanon** worked on the ideas, methodology, supervision, and manuscript review and editing.
- **Paolo Falcone** worked on the ideas, methodology, manuscript review and editing, and managed project funding.

6.4 Paper D

Muhammad Faris, Mario Zanon, Paolo Falcone
A Sensitivity-based Heuristic for Economic Optimal CAVs Coordination in Mixed Traffic at Intersections
Submitted to a peer-reviewed scientific journal.

This paper addresses the problem of coordinating CAVs in mixed traffic with a primary emphasize in economic aspects, such as traffic and energy efficiency. As the problem formulation is cast as Mixed-Integer Nonlinear Program (MINLP), which is intractable for real-time reordering applications, a heuristic algorithm is proposed. Here, two heuristics (EH & SH) are proposed, which consists of feasibility-based pair clustering and (approximate) NLP cost comparison. First, the clustering function narrows down the search area to a subset of promising candidate reorderings; the (approximate) costs associated with the current and alternative sequences are then compared in a search tree to determine the final reordering. As solving multiple NLPs can be more time-consuming, the predictor-corrector QP method is deployed in SH to cheaply approximate NLP solutions. In simulations, it is shown that the performance

of SH and EH can be close to that of MINLP and better than that of FCFS. Here, SH is multiple times faster than EH. Also, as the CAVs penetration rate is reduced, the cost and braking energy consumption can increase.

Individual contributions from each author are listed as follows:

- **Muhammad Faris** worked on the ideas, methodology, programming, and manuscript writing.
- **Mario Zanon** worked on the ideas, methodology, programming (sensitivities acquisition), supervision and manuscript review and editing.
- **Paolo Falcone** was involved in the discussions on the ideas, supervision, manuscript review and editing, and managed project funding.

CHAPTER 7

Conclusions and Future Work

This chapter summarizes the work in this thesis and suggests possible extensions for future research.

Concluding Remarks

This thesis addresses the problem of coordinating CAVs in the presence of HDVs, specifically located at an unsignalized intersection. The setting is therefore regarded as mixed traffic. Indeed, accommodating the non-cooperating HDVs with highly uncertain trajectories introduces challenging problems. These problems are formulated in the form of the research questions **Q1-Q5**.

To indirectly control the HDVs, mixed-platooning strategy is utilized, where a platoon consists of a CAV that happens to be followed by one or more HDVs. The platoon-based CAVs coordination is formulated as an OCP and is regarded as a MIP problem. In simulations, the platooning concept has been proven to be successful to regulate HDVs behavior such that HDVs cannot enter CZ when another vehicle occupies CZ (**Q1**). Additionally, solving exactly MIP problem yields optimal trajectories for the CAVs (**Q2**), albeit it is computationally intractable for real-world applications.

This motivates the development of computationally-efficient heuristic algorithms to obtain approximate solutions in a reasonable amount of time. A feasibility-enforcing ADMM is proposed to retrieve initial solutions which involve the binaries associated with crossing order and collision avoidance constraints. In simulations it can be seen that ADMM can attain near-optimal solutions while multiple times faster than MIQP (**Q3**).

Another consequence of having HDVs in a platoon is that the HDVs may opt to decelerate such that the leading CAV needs to react accordingly. This can trigger a reordering such that the current crossing sequence is swapped by an alternative one which is deemed more optimal or feasible. Again, solving large-size MIP problem in closed-loop scheme to perform reordering is not reasonable.

As a testbed, the reordering problem is studied in a small-scale prioritization problem of a pair of a HDV and a CAV. A heuristic here is built upon the notion that priority has to switch in the case where the HDV behavior is leading to an increase of the cost beyond a prescribed bound. To reduce computational burden, the sensitivity-based approximation technique is exploited to estimate the approximate cost.

To further address reordering in general mixed traffic scenarios, EH is developed by combining collision avoidance constraint violation consistency check and QPs cost comparison (**Q4**). It is shown here that EH can perform reasonably close reordering solutions with the MIQP problem and outperforms the alternative heuristics.

Furthermore, an optimal coordination problem with an emphasis on economic aspects, such as traffic and energy efficiency, is formulated as MINLP and associated EH algorithms are applied (**Q5**). As solving multiple NLPs can be time consuming, SH is then proposed. Here, SH can yield approximate solutions close to EH but several times faster.

Future Work

Toward realizing a safe CAVs coordination in mixed traffic, there are nevertheless many aspects from the work in this thesis that need to be further addressed and developed, which are discussed next.

Hierarchical & Scenario-based approaches: To introduce more flexibilities to the heuristic algorithms when performing in medium to low CAVs pene-

tration rate, an upper-level *configurator* can be deployed. The tasks of this configurator are to assess the possibility of splitting platoons or rearrange constraints against isolated (leading) HDVs depending on current situations. Hence, the structure of MIP problem can be time-varying. The framework can also be extended to include other type of agent, such as Connected HDVs.

Additionally, the driving intention of the HDVs can be explicitly considered in the coordination problem to formulate stochastic-based/ multi-modal approaches.

Data-driven HDV prediction model: While here a simple, least-assumption model to predict HDVs trajectories is employed, a better performance of CAVs coordination can be potentially achieved if instead a more accurate data-driven, learning-based model is utilized. Further, if a scenario-based coordination problem is ever formulated, a multi-modal prediction technique can be used to estimate the direction taken by HDVs at CZ, e.g., turning or going forward.

Continuous flow and more realistic traffic settings: To further develop the heuristics toward generalization, a continuous traffic flow setting, with various HDVs trajectories and stochasticity, can be simulated to see their effectiveness in a more realistic traffic. This can be followed by some practical extensions such as multiple CZs, adjacent intersections, multi-lane, or pedestrian crossing configurations.

Real-world experiments: It is also important to extend the current work toward real-world experimental implementations, where practical issues such as the distribution of algorithms computations to perform in real-time or communication protocols need to be taken care of.

References

[1] A. Alessandrini, A. Campagna, P. D. Site, F. Filippi, and L. Persia, "Automated Vehicles and the Rethinking of Mobility and Cities," *Transportation Research Procedia*, vol. 5, pp. 145–160, 2015.

[2] R. Caudill, A. Kornhauser, and J. Wroble, "Hierarchical vehicle management concept for automated guideway transportation systems," *IEEE Transactions on Vehicular Technology*, vol. 28, no. 1, pp. 11–21, 1979.

[3] S. Huang, A. W. Sadek, and Y. Zhao, "Assessing the Mobility and Environmental Benefits of Reservation-Based Intelligent Intersections Using an Integrated Simulator," *IEEE Transactions on Intelligent Transportation Systems*, vol. 13, no. 3, pp. 1201–1214, 2012.

[4] J. Rios-Torres and A. A. Malikopoulos, "A Survey on the Coordination of Connected and Automated Vehicles at Intersections and Merging at Highway On-Ramps," *IEEE Transactions on Intelligent Transportation Systems*, vol. 18, no. 5, pp. 1066–1077, 2017.

[5] R. Hult, M. Zanon, S. Gros, and P. Falcone, "Primal decomposition of the optimal coordination of vehicles at traffic intersections," *2016 IEEE Conference on Decision and Control (CDC)*, pp. 2567–2573, 2016.

[6] "Taxonomy and Definitions for Terms Related to Driving Automation Systems for On-Road Motor Vehicles," SAE International, Tech. Rep. J3016, 2021.

[7] E.-H. Choi, *Crash Factors in Intersection-Related Crashes: An On-Scene Perspective: (621942011-001)*, Institution: American Psychological Association, 2010.

[8] T. Zhang and J. Wang, "Human reliability analysis of traffic safety," *Lecture Notes in Electrical Engineering*, vol. 259, pp. 491–498, Oct. 2014.

[9] R. Hult, G. R. Campos, E. Steinmetz, L. Hammarstrand, P. Falcone, and H. Wymeersch, "Coordination of Cooperative Autonomous Vehicles: Toward safer and more efficient road transportation," *IEEE Signal Processing Magazine*, vol. 33, no. 6, pp. 74–84, 2016.

[10] J. Li, C. Yu, Z. Shen, Z. Su, and W. Ma, "A survey on urban traffic control under mixed traffic environment with connected automated vehicles," *Transportation Research Part C: Emerging Technologies*, vol. 154, p. 104 258, 2023.

[11] S. Gong and L. Du, "Cooperative platoon control for a mixed traffic flow including human drive vehicles and connected and autonomous vehicles," *Transportation Research Part B: Methodological*, vol. 116, pp. 25–61, 2018.

[12] "National Motor Vehicle Crash Causation Survey: Report to Congress," Tech. Rep. DOT HS 811 059, 2008.

[13] R. Hult, M. Zanon, S. Gros, H. Wymeersch, and P. Falcone, "Optimisation-based coordination of connected, automated vehicles at intersections," *Vehicle System Dynamics*, vol. 58, no. 5, pp. 726–747, 2020.

[14] G. R. Campos, P. Falcone, R. Hult, H. Wymeersch, and J. Sjöberg, "Traffic Coordination at Road Intersections: Autonomous Decision-Making Algorithms Using Model-Based Heuristics," *IEEE Intelligent Transportation Systems Magazine*, vol. 9, no. 1, pp. 8–21, 2017.

[15] A. Katriniok, P. Kleibaum, and M. Joševski, "Distributed Model Predictive Control for Intersection Automation Using a Parallelized Optimization Approach," *IFAC-PapersOnLine*, vol. 50, no. 1, pp. 5940–5946, 2017.

[16] A. M. Mahbub, A. A. Malikopoulos, and L. Zhao, "Decentralized optimal coordination of connected and automated vehicles for multiple traffic scenarios," *Automatica*, vol. 117, p. 108 958, 2020.

[17] A. I. Morales Medina, N. V. D. Wouw, and H. Nijmeijer, "Cooperative Intersection Control Based on Virtual Platooning," *IEEE Transactions on Intelligent Transportation Systems*, vol. 19, no. 6, pp. 1–14, 2018.

[18] H. Xu, Y. Zhang, C. G. Cassandras, L. Li, and S. Feng, "A bi-level cooperative driving strategy allowing lane changes," *Transportation Research Part C: Emerging Technologies*, vol. 120, 2020.

[19] R. Hult, M. Zanon, S. Gras, and P. Falcone, "An MIQP-based heuristic for Optimal Coordination of Vehicles at Intersections," in *2019 IEEE Conference on Decision and Control (CDC)*, 2019, pp. 2783–2790.

[20] S. Kojchev, R. Hult, and J. Fredriksson, "Quadratic approximation based heuristic for optimization-based coordination of automated vehicles in confined areas," in *2022 IEEE Conference on Decision and Control (CDC)*, 2022, pp. 6156–6162.

[21] C. Bali and A. Richards, "Merging Vehicles at Junctions using Mixed-Integer Model Predictive Control," *2018 European Control Conference (ECC)*, pp. 1740–1745, 2018.

[22] A. P. Chouhan and G. Banda, "Autonomous Intersection Management: A Heuristic Approach," *IEEE Access*, vol. 6, pp. 53 287–53 295, 2018.

[23] Z. Shen, A. Mahmood, Y. Wang, and L. Wang, "Coordination of connected autonomous and human-operated vehicles at the intersection," *IEEE/ASME International Conference on Advanced Intelligent Mechatronics, AIM*, vol. 2019-July, pp. 1391–1396, 2019.

[24] A. A. Malikopoulos, C. G. Cassandras, and Y. J. Zhang, "A decentralized energy-optimal control framework for connected automated vehicles at signal-free intersections," *Automatica*, vol. 93, pp. 244–256, 2018.

[25] L. Makarem and D. Gillet, "Model predictive coordination of autonomous vehicles crossing intersections," *IEEE Conference on Intelligent Transportation Systems, Proceedings, ITSC*, pp. 1799–1804, 2013.

[26] H. Xu, Y. Zhang, L. Li, and W. Li, "Cooperative Driving at Unsignalized Intersections Using Tree Search," *IEEE Transactions on Intelligent Transportation Systems*, vol. 21, no. 11, pp. 4563–4571, 2020.

[27] B. Chalaki and A. A. Malikopoulos, "An Optimal Coordination Framework for Connected and Automated Vehicles in two Interconnected Intersections," in *IEEE Conference on Control Technology and Applications (CCTA)*, Hong Kong, 2019, p. 6.

[28] S. Boyd, "Distributed Optimization and Statistical Learning via the Alternating Direction Method of Multipliers," *Foundations and Trends® in Machine Learning*, vol. 3, no. 1, pp. 1–122, 2010.

[29] R. Takapoui, N. Moehle, S. Boyd, and A. Bemporad, "A simple effective heuristic for embedded mixed-integer quadratic programming," *International Journal of Control*, vol. 93, no. 1, pp. 2–12, 2020.

[30] F. Ju, N. Murgovski, W. Zhuang, X. Hu, Z. Song, and L. Wang, "Predictive energy management with engine switching control for hybrid electric vehicle via ADMM," *Energy*, vol. 263, p. 125 971, 2023.

[31] S. East and M. Cannon, "Fast Optimal Energy Management With Engine On/Off Decisions for Plug-in Hybrid Electric Vehicles," *IEEE Control Systems Letters*, vol. 3, no. 4, pp. 1074–1079, 2019.

[32] M. Faris, A. Núñez, Z. Su, and B. De Schutter, "Distributed optimization for railway track maintenance operations planning," in *2018 21st International Conference on Intelligent Transportation Systems (ITSC)*, 2018, pp. 1194–1201.

[33] C. Chen, J. Wang, Q. Xu, J. Wang, and K. Li, "Mixed platoon control of automated and human-driven vehicles at a signalized intersection: Dynamical analysis and optimal control," *Transportation Research Part C: Emerging Technologies*, vol. 127, no. March, p. 103 138, 2021.

[34] B. Peng, M. F. Keskin, B. Kulcsár, and H. Wymeersch, "Connected autonomous vehicles for improving mixed traffic efficiency in unsignalized intersections with deep reinforcement learning," *Communications in Transportation Research*, vol. 1, p. 100 017, 2021.

[35] A. M. Ishtiaque Mahbub and A. A. Malikopoulos, "A Platoon Formation Framework in a Mixed Traffic Environment," *Control Systems Letters, IEEE*, vol. 6, pp. 1–7. 2022.

[36] S. Feng, Z. Song, Z. Li, Y. Zhang, and L. Li, "Robust Platoon Control in Mixed Traffic Flow Based on Tube Model Predictive Control," 2019, arXiv: 1910.07477.

[37] R. Mohebifard and A. Hajbabaie, "Trajectory control in roundabouts with a mixed fleet of automated and human-driven vehicles," *Computer-Aided Civil and Infrastructure Engineering*, pp. 1–19, 2021.

[38] J. Bethge, B. Morabito, H. Rewald, A. Ahsan, S. Sorgatz, and R. Findeisen, "Modelling human driving behavior for constrained model predictive control in mixed traffic at intersections," *IFAC-PapersOnLine*, vol. 53, no. 2, pp. 14 356–14 362, 2020.

[39] M. B. Mertens, J. Muller, and M. Buchholz, "Cooperative Maneuver Planning for Mixed Traffic at Unsignalized Intersections Using Probabilistic Predictions," in *2022 IEEE Intelligent Vehicles Symposium (IV)*, 2022, pp. 1174–1180.

[40] G. N. Bifulco, A. Coppola, A. Petrillo, and S. Santini, "Decentralized cooperative crossing at unsignalized intersections via vehicle-to-vehicle communication in mixed traffic flows," *Journal of Intelligent Transportation Systems*, pp. 1–26, 2022.

[41] R. Hult, G. R. Campos, P. Falcone, and H. Wymeersch, "An approximate solution to the optimal coordination problem for autonomous vehicles at intersections," in *2015 IEEE American Control Conference (ACC)*, 2015, pp. 763–768.

[42] G. R. Campos, A. H. Runarsson, F. Granum, P. Falcone, and K. Alenljung, "Collision avoidance at intersections: A probabilistic threat-assessment and decision-making system for safety interventions," in *2014 IEEE International Conference on Intelligent Transportation Systems (ITSC)*, 2014, pp. 649–654.

[43] E. Sabouni and C. G. Cassandras, "Optimal Merging Control of an Autonomous Vehicle in Mixed Traffic: An Optimal Index Policy," *IFAC-PapersOnLine*, vol. 56, no. 2, pp. 2353–2358, 2023.

[44] R. Hult, M. Zanon, S. Gros, and P. Falcone, "Energy-Optimal Coordination of Autonomous Vehicles at Intersections," in *2018 European Control Conference (ECC)*, 2018, pp. 602–607.

[45] P. Scheffe, G. Dorndorf, and B. Alrifaee, "Increasing Feasibility with Dynamic Priority Assignment in Distributed Trajectory Planning for Road Vehicles," in *2022 IEEE International Conference on Intelligent Transportation Systems (ITSC)*, 2022, pp. 3873–3879.

[46] F. Molinari, A. Katriniok, and J. Raisch, "Real-Time Distributed Automation Of Road Intersections," in *IFAC-PapersOnLine*, vol. 53, 2020, pp. 2606–2613.

[47] B. Chalaki and A. A. Malikopoulos, "A Priority-Aware Replanning and Resequencing Framework for Coordination of Connected and Automated Vehicles," *IEEE Control Systems Letters*, vol. 6, pp. 1772–1777, 2022.

[48] W. Xiao and C. G. Cassandras, "Decentralized Optimal Merging Control for Connected and Automated Vehicles with Optimal Dynamic Resequencing," in *2020 IEEE American Control Conference (ACC)*, 2020, pp. 4090–4095.

[49] A. V. Fiacco, *Introduction to Sensitivity and Stability Analysis in Nonlinear Programming* (Mathematics in Science and Engineering). Elsevier, 1983, vol. 165.

[50] J. B. Rawlings, D. Q. Mayne, and M. M. Moritz, *Model predictive control: Theory, Computation, and Design 2nd Edition*. 2019, vol. 197, Publication Title: Studies in Systems, Decision and Control ISSN: 21984190.

[51] E. Suwartadi, V. Kungurtsev, and J. Jäschke, "Sensitivity-Based Economic NMPC with a Path-Following Approach," *Processes*, vol. 5, no. 4, p. 8, 2017.

[52] V. Kungurtsev and M. Diehl, "Sequential quadratic programming methods for parametric nonlinear optimization," *Computational Optimization and Applications*, vol. 59, no. 3, pp. 475–509, 2014.

[53] M. Conforti, G. Cornuéjols, and G. Zambelli, *Integer Programming* (Graduate Texts in Mathematics). Cham: Springer International Publishing, 2014, vol. 271.

[54] R. Rajamani, *Vehicle Dynamics and Control* (Mechanical Engineering Series). Springer US, 2012.

[55] L. Guzzella, A. Sciarretta, and L. Guzzella, *Vehicle propulsion systems: introduction to modeling and optimization*, 3rd ed. Heidelberg New York: Springer-Verlag, 2013.

[56] M. Faris, P. Falcone, and J. Sjoberg, "Optimization-Based Coordination of Mixed Traffic at Unsignalized Intersections Based on Platooning Strategy," in *2022 IEEE Intelligent Vehicles Symposium (IV)*, 2022, pp. 977–983.

[57] A. M. I. Mahbub and A. A. Malikopoulos, "Platoon Formation in a Mixed Traffic Environment: A Model-Agnostic Optimal Control Approach," in *2022 American Control Conference (ACC)*, 2022, pp. 4746–4751.

[58] P. G. Gipps, "A behavioural car-following model for computer simulation," *Transportation Research Part B*, vol. 15, no. 2, pp. 105–111, 1981.

[59] M. Treiber, A. Hennecke, and D. Helbing, "Congested traffic states in empirical observations and microscopic simulations," *Physical Review E - Statistical Physics, Plasmas, Fluids, and Related Interdisciplinary Topics*, vol. 62, no. 2, pp. 1805–1824, 2000.

[60] M. Bando, K. Hasebe, A. Nakayama, A. Shibata, and Y. Sugiyama, "Dynamical model of traffic congestion and numerical simulation," *Physical Review E*, vol. 51, no. 2, pp. 1035–1042, 1995.

[61] S. Moon and K. Yi, "Human driving data-based design of a vehicle adaptive cruise control algorithm," *Vehicle System Dynamics*, vol. 46, no. 8, pp. 661–690, 2008.

[62] Alejandro Ivan Morales Medina, F. Creemers, E. Lefeber, and N. van de Wouw, "Optimal Access Management for Cooperative Intersection Control," *IEEE Transactions om Intelligent Transportation Systems*, vol. 21, no. 5, pp. 1–26, 2020.

[63] N. Murgovski, L. M. Johannesson, and B. Egardt, "Optimal Battery Dimensioning and Control of a CVT PHEV Powertrain," *IEEE Transactions on Vehicular Technology*, vol. 63, no. 5, pp. 2151–2161, 2014.

[64] M. Zanon and T. Faulwasser, "Economic MPC without terminal constraints: Gradient-correcting end penalties enforce asymptotic stability," *Journal of Process Control*, vol. 63, pp. 1–14, 2018.

[65] J. Nocedal and S. Wright, *Numerical Optimization*. Springer New York, 2006, Series Title: Springer Series in Operations Research and Financial Engineering.

[66] P. Bonami and J. Lee, "BONMIN User's manual," 2011.

[67] A. Wächter and L. T. Biegler, "On the implementation of an interior-point filter line-search algorithm for large-scale nonlinear programming," *Mathematical Programming*, vol. 106, no. 1, pp. 25–57, 2006.